UNIVERSIDADE FEDERAL DA FRONTEIRA SUL

***CAMPUS* CERRO LARGO**

PROGRAMA DE PÓS-GRADUAÇÃO EM AMBIENTE E TECNOLOGIAS SUSTENTÁVEIS

LEANDRO PELLENZ

ESTUDO DO TRATAMENTO DE LIXIVIADO DE ATERRO SANITÁRIO POR UM SISTEMA FOTO-ELETRO-FENTON INTEGRADO COM OXIDAÇÃO BIOLÓGICA

CERRO LARGO

2020

LEANDRO PELLENZ

ESTUDO DO TRATAMENTO DE LIXIVIADO DE ATERRO SANITÁRIO POR UM SISTEMA FOTO-ELETRO-FENTON INTEGRADO COM OXIDAÇÃO BIOLÓGICA

Dissertação de mestrado apresentada ao Programa de Pós-Graduação em Ambiente e Tecnologias Sustentáveis da Universidade Federal da Fronteira Sul, como requisito parcial para obtenção do título de Mestre em Ambiente e Tecnologias Sustentáveis

Linha de Pesquisa: Desenvolvimento de Processos e Tecnologias

Orientador: Prof. Dr. Fernando Henrique Borba

Coorientador: Prof. Dr. Daniel Joner Daroit

CERRO LARGO

2020

FICHA CATALOGRÁFICA

Bibliotecas da Universidade Federal da Fronteira Sul - UFFS

Pellenz, Leandro
ESTUDO DO TRATAMENTO DE LIXIVIADO DE ATERRO SANITÁRIO POR UM SISTEMA FOTO-ELETRO-FENTON INTEGRADO COM OXIDAÇÃO BIOLÓGICA / Leandro Pellenz. -- 2020.
204 f.

Orientador: Dr. Fernando Henrique Borba.
Co-orientador: Dr. Daniel Joner Daroit.
Dissertação (Mestrado) - Universidade Federal da Fronteira Sul, Programa de Pós-Graduação em Ambiente e Tecnologias Sustentáveis-PPGATS, Cerro Largo, RS , 2020.

1. Foto-eletro-Fenton. 2. Processos oxidativos avançados. 3. Oxidação biológica. 4. Lixiviado de aterro sanitário. 5. Toxicidade. I. Borba, Fernando Henrique, orient. II. Daroit, Daniel Joner, co-orient. III. Universidade Federal da Fronteira Sul. IV. Título.

Elaborada pelo sistema de Geração Automática de Ficha de Identificação da Obra pela UFFS com os dados fornecidos pelo(a) autor(a).

LEANDRO PELLENZ

ESTUDO DO TRATAMENTO DE LIXIVIADO DE ATERRO SANITÁRIO POR UM SISTEMA FOTO-ELETRO-FENTON INTEGRADO COM OXIDAÇÃO BIOLÓGICA

Dissertação de Mestrado, apresentada ao Programa de Pós-Graduação em Ambiente e Tecnologias Sustentáveis da Universidade Federal da Fronteira Sul, como requisito parcial para a obtenção do título de Mestre em Ambiente e Tecnologias Sustentáveis.

Área de Concentração: Tratamento de Efluentes
Linha de Pesquisa: Desenvolvimento de Processos e Tecnologias

Orientador: Prof. Dr. Fernando Henrique Borba
Coorientador: Prof. Dr. Daniel Joner Daroit

Esta Dissertação foi defendida e aprovada pela banca em: 19/02/2020

BANCA EXAMINADORA

Prof. Dr. Bruno Munchen Wenzel

Prof. Dr. Adriano da Silva

Prof. Dr. Fernando Henrique Borba

Dedico aos meus pais, pelo apoio e investimento na busca dos meus objetivos.

AGRADECIMENTOS

Aos meus pais, Eliseu Inácio Pellenz e Vera Lúcia Moellmann Pellenz, pelo incondicional apoio, preocupação e incentivo do início ao fim de mais esta etapa da minha vida.

Ao meu irmão, Marcos Roberto Pellenz, pela parceria e suporte, sempre que necessário.

Ao meu orientador e amigo, Professor Dr. Fernando Henrique Borba, por todos os valiosos ensinamentos, conselhos, apoio, amizade e principalmente por me abrir portas para a pesquisa.

Ao meu co-orientador Professor Dr. Daniel Joner Daroit, por todos ensinamentos e conselhos, e pelas oportunidades, desde minha iniciação científica na graduação, até a conclusão do presente trabalho.

Aos meus amigos e colegas de pesquisa Francine Bueno, Jonas Jean Inticher, Michely Schmitz, Daiana Seibert, Raíssa Engroff Guimarães e Camila Zorzo, pelo auxílio neste trabalho.

Aos Professores do Programa de Pós-Graduação em Ambiente e Tecnologias Sustentáveis, pelos pelo auxílio na minha formação.

Aos colegas do Programa de Pós-Graduação em Ambiente e Tecnologias Sustentáveis, pela parceria, em especial aos meu amigos e colegas de moradia, Lucas Adriano Pachla e Manoel Francisco Mendes Lassen.

Aos técnicos dos laboratórios da Universidade Federal da Fronteira Sul, campus Cerro Largo, pelo apoio prestado.

Ao Programa de Pós-Graduação em Engenharia Química da Universidade Estadual do Oeste do Paraná - UNIOESTE, campus Toledo-PR, pela disponibilidade dos laboratórios e equipamentos.

À FAPERGS/CAPES, pela concessão da bolsa de mestrado.

À Universidade Federal da Fronteira Sul, sua direção, seus servidores, técnicos e docentes pelo suporte prestado e principalmente pela oportunidade de realização deste mestrado.

A todos que de alguma forma contribuíram ao longo desta minha jornada.

RESUMO

Devido ao seu alto potencial poluidor, características tóxicas e recalcitrância, lixiviados de aterro sanitário (LAS) demandam tratamento adequado antes do seu descarte no meio ambiente, a fim de proteger a saúde pública e conservar os ecossistemas. Em razão da eficiência e aplicabilidade limitada de processos convencionais no tratamento de LAS, se torna importante a investigação, caracterização e aperfeiçoamento de técnicas avançadas de tratamento, visando reduzir efeitos tóxicos e degradar compostos recalcitrantes, aumentando a sua biodegradabilidade. Este trabalho investigou a performance dos processos foto-eletro-Fenton (FEF) e oxidação biológica (OB) aeróbia integrados na degradação de LAS. Ambos foram avaliados em escala laboratorial, usando reatores batelada. As melhores condições experimentais de concentração de H_2O_2, intensidade de corrente, e vazão do sistema FEF, em 15 minutos de processo, foram obtidas através de uma metodologia de superfície de resposta, sendo 300 mg H_2O_2 L^{-1}, 0,9 A e 0,6 L min^{-1}, respectivamente. O processo de OB foi conduzido por 72 horas, utilizando lodo ativado de uma indústria de laticínios. A estratégia de tratamento aplicando processo FEF seguido de OB demonstrou a melhor performance, atingindo reduções de 77,9%, 71,5% e 76,3% de demanda química de oxigênio (DQO), carbono total (CT) e absorbância de radiação em 254 nm (Abs 254 nm), respectivamente. Foram observadas significativas reduções na genotoxicidade (*Allium cepa*) com um aumento de 131,5% do índice mitótico e uma diminuição de 47,8% das anormalidades, além de reduções da fitotoxicidade (*Lactuca sativa*), verificadas pelo aumento dos índices de germinação e redução da inibição do crescimento das plantas. A integração dos sistemas promoveu a degradação de contaminantes emergentes identificados no LAS bruto, com destaque para o Bisfenol-A (BPA). Desta forma, o sistema proposto de FEF seguido de OB se apresenta como uma alternativa relevante, de boa eficiência para a remoção de poluentes presentes em LAS, com potencial de aplicação na minimização dos impactos ambientais causados por este efluente.

Palavras-chave: Foto-eletro-Fenton, processos oxidativos avançados, oxidação biológica, lixiviado de aterro sanitário, toxicidade.

ABSTRACT

Due to its high polluting potential, toxic characteristics and recalcitrance, landfill leachates (LL) demand an adequate treatment before its disposal in the environment, in order to protect public health and conserve ecosystems. In face of the limited efficiency and applicability of conventional treatment processes in the treatment of LL, the investigation, characterization and improvement of advanced techniques become important, aiming to reduce the toxic effects and degrade recalcitrant compounds, increasing its biodegradability. This research investigated the performance of the photo-electro-Fenton (FEF) and aerobic biological oxidation (BO) processes integrated in the degradation of LL. Both processes were assessed in lab scale, using batch reactors. The best experimental conditions of H_2O_2 concentration, current intensity and flow rate of the PEF system, in 15 min of process, were obtained through a response surface methodology, resulting in 300 mg H_2O_2 L^{-1}, 0.9 A and 0.6 L min^{-1}, respectively. The BO processes was carried out for 72 hours, using activated sludge from a dairy industry. The strategy that applied the PEF process followed by BO showed the best performance, reaching reductions of 77.9%, 71.5% e 76.3%, in chemical oxygen demand (COD), total carbon (TC) and radiation absorbance in 254 nm (Abs 254 nm), respectively. Additionally, significant reductions in genotoxicity (*Allium cepa*) were observed by an increase of 131.5% in the mitotic index and a decrease of 47.8% in the abnormalities, besides reductions in the phytotoxicity (*Lactuca sativa*), verified by the increase in the germination rates and reduction in the plant growth inhibition. The integration of the systems promoted degradation of emerging contaminants identified in the raw LL, highlighting Bisphenol-A (BPA). Thus, the proposed system of PEF followed by BO is presented as a relevant alternative, having good efficiency in the removal of pollutants present in LL, with potential for application in the minimization of the environmental impacts caused by this effluent.

Keywords: Photo-electro-Fenton, advanced oxidation processes, biological oxidation, landfill leachate, toxicity.

LISTA DE FIGURAS

LISTA DE TABELAS

LISTA DE SIGLAS E ABREVIATURAS

$^{\bullet}OH$	hidroxila
Abs 254 nm	absorbância de radiação em 254 nm
BPA	bisfenol A
BDD	diamante dopado com boro
CG-EM	cromatografia gasosa – espectrometria de massas
CO_2	dióxido de carbono
COT	carbono orgânico total
DBO	demanda bioquímica de oxigênio
DQO	demanda química de oxigênio
FEF	foto-eletro-Fenton
H_2O_2	peróxido de hidrogênio
$HO_2^{\bullet}$	hidroperoxil
LAS	lixiviado de aterro sanitário
O_2	oxigênio
OB	oxidação biológica
PEOAs	processos eletro-oxidativos avançados
POAs	processos oxidativos avançados
RSU	resíduos sólidos urbanos
ST	sólidos totais
UVC	ultravioleta C

LISTA DE SIGLAS E ABREVIATURAS – ARTIGO (inglês)

$^{\bullet}OH$	hydroxyl
Abs 254 nm	radiation absorbance in 254 nm
BO	biological oxidation
BPA	bisphenol A
BDD	boron-doped diamond
CCRD	central composite rotational design
COD	chemical oxygen demand
DBA	2,6-Dimethoxybenzoic acid
DEET	N,N-Diethyl-3-methylbenzamide
DIOP	Diisooctyl phthalate
EAOPs	electrochemical advanced oxidation processes
EDC	endocrine disruptor chemical
GC-MS	gas chromatography – mass spectrometry
GI	germination index
H_2SO_4	sulfuric acid
HGRI	hypocotyl growth relative inhibition
LL	landfill leachate
MI	mitotic index
NaOH	sodium hydroxide
O_2	oxygen
OD	optical density
PEF	photo-electro-Fenton
RGRI	root growth relative inhibition

ROP	reactor operation parameters
RSM	response surface methodology
RT	retention time
TC	total carbon
TN	total nitrogen
TXRF	total Reflection X-ray Fluorescence
UVC	ultraviolet C

SUMÁRIO

1. INTRODUÇÃO

Atualmente o método mais utilizado de disposição final de resíduos sólidos urbanos (RSU) e rejeitos, no Brasil e no mundo, são os aterros sanitários (BING et al., 2016; DEUS; BATTISTELLE; SILVA, 2017). Nos aterros ocorre, de maneira controlada, decomposição dos resíduos por processos físicos, químicos e biológicos, minimizando os seus potenciais impactos sobre o meio ambiente e a saúde humana (RENOU et al., 2008).

O lixiviado de aterro sanitário (LAS) é o principal subproduto da decomposição de resíduos em aterros, e devido as suas características, seu tratamento é um dos principais desafios relacionados à gestão dos aterros sanitários (MIAN et al., 2017). O LAS pode ter uma composição variada, mas é geralmente caracterizado por conter uma alta carga orgânica, com uma grande variedade de poluentes, incluindo contaminantes emergentes, com frações recalcitrantes e alta toxicidade ao meio ambiente (NAVEEN et al., 2017; SEIBERT et al., 2019a). Devido à essas características, e as significativas quantidades geradas, o LAS é considerado um dos mais importantes problemas ambientais da atualidade, com grande potencial de contaminação de solos e águas superficiais e subterrâneas (BADERNA; CALONI; BENFENATI, 2019).

Processos convencionais de tratamento de efluentes, tais como os biológicos são comumente usados no tratamento de efluentes em geral, devido à sua simplicidade e bom custo-benefício na remoção de compostos orgânicos biodegradáveis. Entretanto, processos biológicos podem ter sua eficiência e aplicabilidade limitada no tratamento de LAS devido à presença de substâncias tóxicas aos microrganismos sua composição e a sua baixa biodegradabilidade, representada pela fração de demanda bioquímica de oxigênio em relação a demanda química de oxigênio (DBO_5/DQO) (PENG, 2017; ZAZOULI et al., 2012).

Devido a isso, surgem como alternativa os processos oxidativos avançados (POAs), que se destacam por seu alto potencial de oxidação de compostos e baixa seletividade, podendo ser aplicados em substituição ou integrados a processos convencionais (OLLER; MALATO; SÁNCHEZ-PÉREZ, 2011). POAs se caracterizam pela geração *in situ* de radicais com alto potencial de oxidação, que realizam a

degradação mineralização de compostos, convertendo-os em CO_2, água e íons inorgânicos.

Existem várias classes e mecanismos de funcionamento de POAs, com destaque para os baseados na geração de radicais hidroxila ($^{\bullet}OH$). Na produção de radicais $^{\bullet}OH$ são comumente usados os processos baseados na reação Fenton, que consiste na decomposição de peróxido de hidrogênio (H_2O_2) por íons de Fe^{2+} (WANG et al., 2016). O processo Fenton pode apresentar grande eficiência na remoção de poluentes, especialmente quando combinado com outros mecanismos, como corrente elétrica (eletro-Fenton) e radiação (foto-Fenton) ou a combinação de ambos, denominada foto-eletro-Fenton (FEF) (BRILLAS; SIRÉS; OTURAN, 2009; MOREIRA et al., 2017).

Diversas variáveis, bem como a relação entre estas variáveis, podem influenciar a eficiência do processo FEF no tratamento de LAS, tais como a composição e concentração de carga orgânica do efluente, as concentrações dos reagentes H_2O_2 e Fe^{2+}, a intensidade/densidade de corrente elétrica, o material dos eletrodos, a presença de O_2 dissolvido, o pH da solução, entre outros (MOREIRA et al., 2017; UMAR; AZIZ; YUSOFF, 2010). Assim, é de fundamental importância que estes parâmetros sejam estudados, buscando a máxima eficiência de degradação/mineralização de poluentes para cada sistema proposto.

Visando um estudo mais amplo da eficácia de POAs na minimização dos impactos ambientais causados por LAS, pesquisadores tem investigado – além dos parâmetros convencionais, tais como demanda química de oxigênio (DQO), demanda bioquímica de oxigênio (DBO) e carbono orgânico total (COT) – parâmetros como toxicidade ambiental, utilizando bioindicadores, e subprodutos, com o objetivo de identificar compostos que, mesmo em pequenas quantidades, podem causar efeitos tóxicos severos ao meio ambiente (BORBA et al., 2018; DE PAULI et al., 2018; SEIBERT et al., 2019b).

1.1 OBJETIVOS

1.1.1 Objetivo geral

Investigar a performance de um sistema FEF integrado a OB na degradação de LAS.

1.1.2 Objetivos específicos

- Realizar uma caracterização físico química do LAS bruto e tratado nas diferentes condições estudadas.
- Investigar as melhores condições experimentais de um sistema FEF no tratamento de LAS, comparando ânodos de BDD com ânodos de ferro doce.
- Avaliar a integração do sistema FEF com um processo de OB aeróbia.
- Realizar ensaios de fitotoxicidade (*Lactuca sativa*) e genotoxicidade (*Allium cepa*) no LAS bruto e tratado.
- Realizar análise de metais e subprodutos no LAS bruto e tratado.

1.1.3 Estrutura do trabalho

A presente dissertação foi dividida em três capítulos, sendo o primeiro de introdução, apresentando uma contextualização geral acerca do problemática do LAS e de possíveis soluções a serem propostas. O segundo capitulo apresenta uma revisão bibliográfica sobre a geração de LAS, suas características e alternativas de tratamento. O terceiro capítulo é dedicado à exposição do artigo científico produzido a partir do presente trabalho e submetido à revista *Journal of Environmental Management*, com detalhamento da metodologia, dados experimentais e discussão dos resultados.

2 REVISÃO BIBLIOGRÁFICA

Este capítulo busca apresentar o embasamento para o desenvolvimento da pesquisa. Inicia-se com uma revisão sobre a geração e disposição final RSU, passando pela geração de LAS e suas características, bem como as técnicas de tratamento deste efluente. Dentre as alternativas de tratamento, é realizada uma abordagem mais aprofundada acerca de processos biológicos aeróbios e POAs baseados na reação Fenton.

2.1 RESÍDUOS SÓLIDOS

A maior parte das atividades humanas gera resíduos, tanto na produção quanto no consumo de bens e serviços. Os RSU são uma das maiores e mais importantes classes de resíduos, sendo classificados pela Política Nacional dos Resíduos Sólidos como (i) resíduos domiciliares: provenientes de atividades domésticas e (ii) resíduos de limpeza urbana: originários de limpeza de áreas e vias públicas (BRASIL, 2010). Estes resíduos possuem uma composição bastante variada, com destaque para resíduos alimentares, plástico, papel/papelão, metal, vidro, resíduos de jardinagem, entre outros (EDJABOU et al., 2015).

De acordo com o Banco Mundial são gerados diariamente no mundo 0,74 kg per capita de resíduos sólidos, sendo que esta taxa varia de 0,11 até 4,54 entre países de acordo com os níveis de renda da população. No ano de 2016 foram gerados aproximadamente 2,01 bilhões de toneladas de resíduos sólidos no mundo, e estima-se que em 2050 este número atinja 3,40 bilhões de toneladas anuais (KAZA et al., 2018). No Brasil, dados da Associação Brasileira de Empresas de Limpeza Pública e Resíduos Especiais reportam que a geração de RSU no ano de 2017 foi de 71,6 milhões de toneladas, representando uma geração diária de 1,035 kg per capita (ABRELPE, 2017).

2.1.1 Disposição de resíduos

Devido ao seu bom custo-benefício ambiental em relação a outras alternativas, como compostagem, incineração e disposição em lixões, aterros sanitários são a tecnologia mais utilizada para a disposição final de resíduos sólidos no brasil e mundo

(BING et al., 2016; DEUS; BATTISTELLE; SILVA, 2017). A disposição em aterros pode ser aplicada como tecnologia única de destinação de resíduos, bem como combinada com outras tecnologias para redução do volume final dos resíduos, visando aumentar a eficiência e reduzir os custos do processo (KHAN; FAISAL, 2008; RENOU et al., 2008).

Em torno de 46% dos resíduos sólidos produzidos no mundo tem sua destinação final feita em algum tipo de aterro, enquanto 41% ainda são dispostos de forma aberta em solo (ver Figura 1A) (KAZA et al., 2018).

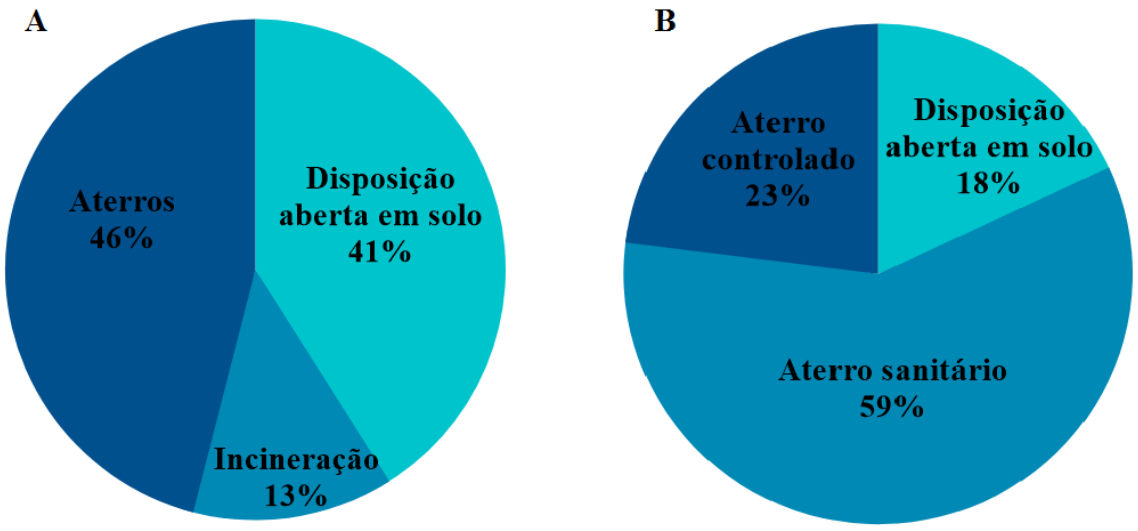

Figura 1. Destinação dos RSU (A) e no Brasil (B) (Adaptado de ABRELPE, 2017; KAZA et al., 2018).

Já no Brasil, onde aproximadamente 90% dos RSU são coletados, 59% são dispostos em aterros sanitários, 23% em aterros controlados e 18% em lixões (ver Figura 1B) (ABRELPE, 2017).

2.1.2 Aterro sanitário

Aterros sanitários consistem em uma forma de disposição de resíduos em células no solo, devidamente impermeabilizadas, com camadas de resíduos sendo dispostas intercaladas com camadas de solo, acompanhado de controle e monitoramento de efluentes gasosos, além da coleta do efluente líquido, que consiste no LAS. Este método possui como principais vantagens o baixo custo e a grande

capacidade de absorção diária de resíduos em comparação com outros métodos, sendo considerado como adequado pela Política Nacional dos Resíduos Sólidos (BRASIL, 2010). Ainda, a Norma Brasileira NBR nº 8419 de 1992, define aterro sanitário de RSU como:

> A técnica de disposição de resíduos sólidos urbanos no solo, sem causar danos à saúde pública e à sua segurança, minimizando os impactos ambientais, método este que utiliza princípios de engenharia para confinar os resíduos sólidos à menor área possível e reduzi-los ao menor volume permissível, cobrindo-os com uma camada de terra na conclusão de cada jornada de trabalho, ou a intervalos menores, se necessário (ABNT, 1992 p.1).

2.2 LIXIVIADO DE ATERRO SANITÁRIO

LAS, juntamente com biogás, são os dois subprodutos liberados durante o processo de decomposição de resíduos sólidos em aterros. O LAS é um efluente aquoso proveniente da percolação da água da chuva nos aterros, umidade dos resíduos e de processos bioquímicos de decomposição dos resíduos que ocorrem nos aterros (RENOU et al., 2008).

2.2.1 Características do LAS

Estes efluentes são caracterizados por uma composição bastante variada, influenciada por diversos fatores, tais como o tipo de resíduos em decomposição, condições climáticas e hidrologia local do aterro, idade do aterro, design e forma de operação do aterro (KULIKOWSKA; KLIMIUK, 2008; ZIYANG et al., 2009). Apesar da grande variabilidade de composição do LAS, estes normalmente se destacam por conter grandes quantidades me matéria orgânica, composta de ácidos húmicos e fúlvicos, hidrocarbonetos aromáticos policíclicos, ésteres, ente outros; além de compostos inorgânicos como cloretos, sulfatos, bicarbonatos, carbonatos, sulfuretos, metais alcalinos e alcalinos terrosos, ferro, manganês espécies nitrogenadas em grandes concentrações e metais pesados (KULIKOWSKA; KLIMIUK, 2008; ÖMAN; JUNESTEDT, 2008)

Na Tabela 1, são listados alguns parâmetros comumente avaliados em LAS por pesquisadores e suas respetivas faixas de valores.

Tabela 1 - Caracterização físico-química de LAS descrita na literatura.

Parâmetro	**Unidade**	**Faixa de valores**
pH	Escala Sörensen	6,4 – 8,61
Condutividade	mS cm^{-1}	2,3 – 41,5
Sólidos totais (ST)	mg L^{-1}	5000 – 11084
Demanda bioquímica de oxigênio (DBO)	mg O_2 L^{-1}	67 – 701
Demanda química de oxigênio (DQO)	mg O_2 L^{-1}	250 – 7125
DBO/DQO	-	0,036 – 0,35
Cor	mg Pt-Co L^{-1}	1944 – 4050
Turbidez	NTU	149 – 4500
Cloro, CL^-	mg L^{-1}	360 – 4900
Flúor, F^-	mg L^{-1}	0,34 – 12
Sulfato, SO_4^{2-}	mg L^{-1}	22 – 650
Bicarbonato, HCO_3^-	mg L^{-1}	300– 5100
Fenóis	mg L^{-1}	0,35 – 10,5
Ferro total	mg L^{-1}	0,6 – 29,5
N – Total	mg L^{-1}	54 – 4368,2
P – Total	mg L^{-1}	0,13 – 43

Fonte: Adaptado de AZIZ et al., 2010; KULIKOWSKA; KLIMIUK, 2008; ÖMAN; JUNESTEDT, 2008; SEIBERT et al., 2019b; ZIYANG et al., 2009.

2.3 TRATAMENTO DE LAS

Devido às características do LAS, seu tratamento normalmente é complexo, não sendo possível a sua realização apenas por métodos convencionais, sendo muitas vezes necessário mais de um processo. Serdarevic (2018) dividiu as técnicas mais aplicadas no tratamento de LAS em cinco grupos:

- Transferência de LAS: recirculação no próprio aterro ou transferência para uma estação de tratamento de esgotos;
- Processos biológicos: processos aeróbios e/ou anaeróbios;
- Processos físico-químicos: oxidação química, adsorção, precipitação química, coagulação, floculação, arraste de ar;
- Processos de membrana: osmose reversa, membrana combinada com tratamento biológico, ultrafiltração, nanofiltração;
- Processos térmicos: evaporação.

A revisão bibliográfica do presente estudo abordará as técnicas de oxidação biológica aeróbia e POAs baseados na reação Fenton, que são alvos desta pesquisa.

2.3.1 Processo de OB aeróbia

Processos biológicos de tratamento de águas residuárias em geral, tanto aeróbios quanto anaeróbios, são baseados na degradação de poluentes por meio de oxidação promovida por microrganismos, sendo geralmente aplicados a efluentes com altos teores de DBO (PENG, 2017). Devido à sua simplicidade operacional e boa relação custo-benefício, estes processos, em conjunto com outras técnicas, são uma das alternativas mais utilizadas para a remoção de carga orgânica e nutrientes de LAS (RENOU et al., 2008). Nos biorreatores os microrganismos podem estar suspensos no efluente a ser tratado, requerendo agitação, ou presos a um suporte sólido, pelo qual o líquido passa durante o processo (HENZE et al., 2008).

Na OB aeróbia, ou seja, na presença de oxigênio (O_2) em solução, a degradação dos compostos orgânicos gera como principais subprodutos dióxido de carbono (CO_2) e lodo (RENOU et al., 2008). Bateladas sequenciais e lodos ativados e lagoas aeradas são as técnicas mais utilizadas de tratamento biológico de LAS. Nas bateladas sequencias, grânulos aeróbios são utilizados em ciclos sequencias, incluindo aeração, sedimentação e descarte. Nos sistemas com lodos ativados, um lodo rico em microrganismos é inserido na solução, na presença de O_2, flocos microbianos são suspensos na solução e promovem a oxidação da matéria orgânica. Lagoas aeradas são geralmente compartimentos maiores de deposição de LAS em que é realizada aeração mecânica, visando promover a atividade dos microrganismos presentes no meio (HENZE et al., 2008; KURNIAWAN et al., 2010; REN et al., 2017).

Grande parte dos microrganismos atuantes na OB são bactérias, de diversas espécies diferentes, podendo ser heterotróficas ou autotróficas. Em processos aeróbios, bactérias heterotróficas são responsáveis pela remoção da DBO, pois obtêm energia predominantemente pela degradação de compostos orgânicos. Nestes processos as bactérias autotróficas fazem a oxidação de compostos inorgânicos, com destaque para as nitrificantes, que utilizam amônio e nitrato como doadores de elétrons. (DAVIES, 2005; GRADY JR et al., 2011).

2.3.1.1 Crescimento microbiano

Em processos do tipo batelada, o crescimento microbiano em um meio rico em nutrientes utilizáveis ocorre em quatro fases principais, conforme apresentado na Figura 2.

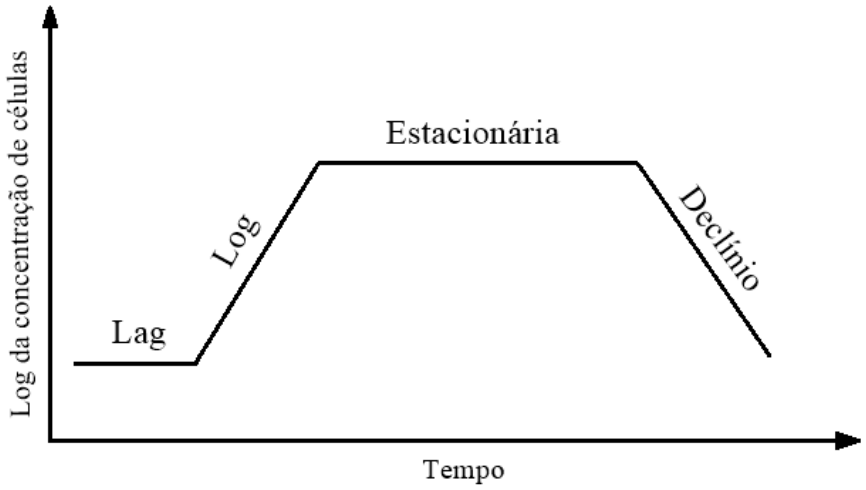

Figura 2. Curva de crescimento microbiano em sistemas fechados (Adaptado de MADIGAN et al., 2016).

Na fase Lag ou fase de adaptação há uma grande quantidade de nutrientes no meio e bactérias possuem alta atividade metabólica e síntese de enzimas, porém ocorre pouca divisão celular. Já durante a fase Log ou fase exponencial inicia-se a divisão celular e a população microbiana entra em um período de crescimento e intensa atividade metabólica. Na sequência inicia a fase estacionária, em que a taxa de morte celular é equivalente à taxa de divisão, mantendo um número aproximadamente constante de microrganismos. Nesse estágio a atividade

metabólica é reduzida, assim como a disponibilidade de nutrientes e ocorre um acúmulo de subprodutos da degradação. Em determinado momento os nutrientes disponíveis no meio tornam se escassos e se inicia a fase de declínio, em que a taxa de morte excede a taxa de divisão celular. A duração e de cada fase, bem como a inclinação das curvas pode variar de acordo com as características da população microbiana e do meio (HENZE et al., 2008; MADIGAN et al., 2016).

2.3.1.2 Biodegradabilidade

A biodegradabilidade de um efluente está relacionada à facilidade/velocidade com que os microrganismos conseguem degradar seus constituintes e também à fração da sua carga orgânica que pode ser efetivamente biodegradada. O COT presente em uma água residuária pode ser dividido em não oxidável e quimicamente oxidável, representado pelo parâmetro DQO. O carbono oxidável divide-se em biorrefratário e biologicamente oxidável ou biodegradável, representado pelo parâmetro DBO. A fração biodegradável da matéria orgânica pode ainda ser dividida em DBO de difícil e fácil degradação. A DBO de difícil degradação composta por moléculas grandes e mais complexas, presente geralmente na forma particulada no efluente, demandando de um tempo de adaptação dos microrganismos horas ou até dias para sua degradação. Por outro lado, a DBO de fácil degradação engloba moléculas pequenas, geralmente na forma solúvel, podendo ser imediatamente consumida por microrganismos heterotróficos (Ver Figura 3) (DAVIES, 2005; LAPERTOT; PULGARIN, 2006).

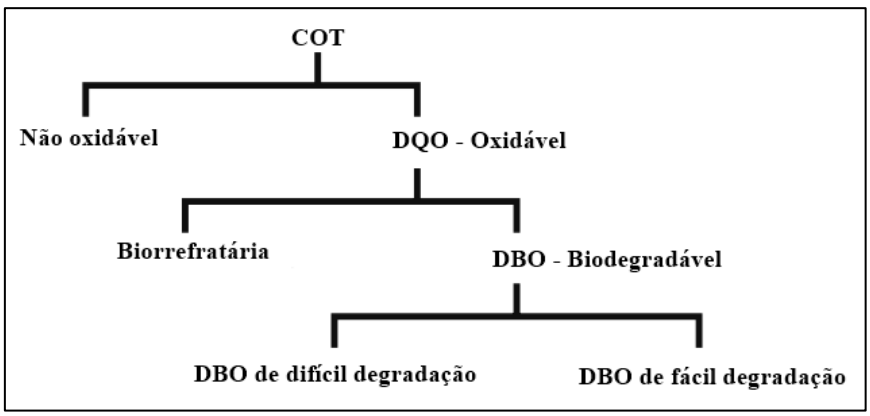

Figura 3. Frações de carbono orgânico e águas residuárias (Adaptado de DAVIES, 2005).

O conhecimento da biodegradabilidade de um efluente é fundamental para a avaliação da aplicabilidade de um processo de tratamento biológico, bem como da eventual necessidade da complementação com um processo físico-químico de pré ou pós tratamento (DAVIES, 2005). Uma das principais formas de avaliar a tratabilidade biológica de um efluente é através da relação DQO/DBO, que representa a razão da quantidade total de matéria orgânica oxidável presente na solução pela quantidade de matéria orgânica biologicamente oxidável (ver Figura 3) (JARDIM; CANELA, 2004).

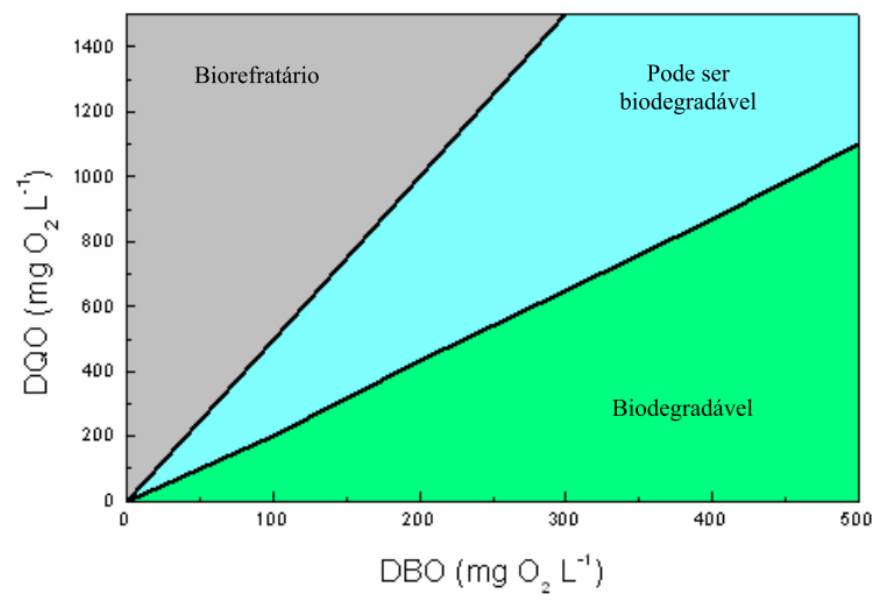

Figura 4. Biodegradabilidade de um efluente a partir da relação DBO/DQO (JARDIM; CANELA, 2004).

Efluentes com razões DQO/DBO menores que 2,5 são considerados facilmente biodegradáveis. Razões DQO/DBO entre 2,5 e 5,0 conferem ao efluente características de biodegradação mais complexa, enquanto razões com DQO/DBO maiores que 5,0 o efluente passa a ser considerado biorefratário (JARDIM; CANELA, 2004). Lixiviados de aterro sanitário em geral contém uma quantidade significativa de compostos recalcitrantes à biodegradação, e além disso, podem conter compostos tóxicos aos microorganismos, sendo este outro importante fator limitante ao tratamento biológico (NAVEEN et al., 2017; RENOU et al., 2008).

2.3.2 Processos oxidativos avançados

Processos oxidativos avançados (POAs) aplicados ao tratamento de águas e efluentes têm recebido crescente atenção da comunidade científica nas últimas décadas, por serem promissores na remoção de compostos recalcitrantes à processos convencionais (BRILLAS; SIRÉS; OTURAN, 2009). POAs englobam uma série de métodos tais como ozonização, fotocatálise, oxidação eletroquímica, e processos baseados na reação Fenton (ASGHAR; ABDUL RAMAN; WAN DAUD, 2015). Estes processos podem usar diferentes sistemas reacionais, mas de modo geral são caraterizados por visar a produção *in situ* de agentes oxidantes altamente reativos, principalmente, mas não exclusivamente, radicais $^{\bullet}OH$ (BRILLAS; SIRÉS; OTURAN, 2009).

O radical $^{\bullet}OH$ é o segundo agente oxidante mais forte conhecido com potencial de redução E° = 2,73 V, podendo degradar a grande maioria dos poluentes orgânicos e organometálicos em CO_2, água e íons inorgânicos (ALLEN J. BARD, ROGER PARSONS, 1985). Radicais $^{\bullet}OH$ podem atacar moléculas de três diferentes modos: (*i*) abstração de um átomo de hidrogênio para a formação de água, (*ii*) hidroxilação ou adição eletrofílica a uma ligação não saturada, (*iii*) transferência de elétrons ou reações redox (BRILLAS; SIRÉS; OTURAN, 2009).

2.3.2.1 Reação Fenton

A reação Fenton, que foi reportada pela primeira vez por Fenton (FENTON, 1894) e descrita de maneira mais detalhada por Haber e Weiss (HABER; WEISS, 1934), promove a produção de ($^{\bullet}OH$). A reação ocorre a partir da transferência de um elétron entre peróxido de hidrogênio (H_2O_2) e um íon ferroso (Fe^{2+}), que atua como catalisador, de acordo com a Equação 1(GALLARD; DE LAAT; LEGUBE, 1998).

$$Fe^{2+} + H_2O_2 \rightarrow Fe^{3+} + {}^{\bullet}OH + OH^{-} \quad (1)$$

O processo se torna mais eficiente em meio ácido, com pH ótimo entre 2,8 e 3,0, devido ao balanço catalítico da fração Fe^{3+}/Fe^{2+} que ocorre nestas condições. Fe^{2+} pode ser regenerado a partir da reação entre Fe^{3+} e H_2O_2, conforme a Equação 2 (HABER; WEISS, 1934).

$$Fe^{3+} + H_2O_2 \rightarrow Fe^{2+} + HO_2^{\bullet} + H^+ \quad (2)$$

Além disso pode ocorrer uma transformação de Fe^{3+} no complexo $[Fe^{III}(HO_2)]^{2+}$ e posterior conversão em radicais hidroperoxila ($HO_2^{\bullet}$) e Fe^{2+} (Eqs. 3 e 4) (DE LAAT; GALLARD, 1999). Radicais $HO_2^{\bullet}$ são significativamente mais seletivos e menos reativos que os radicais $^{\bullet}OH$, com um potencial de redução E° = 1,65 V (ALLEN J. BARD, ROGER PARSONS, 1985).

$$Fe^{3+} + H_2O_2 \leftrightarrow [Fe^{III}(HO_2)]^{2+} + H^+ \quad (3)$$

$$[Fe^{III}(HO^2)]^{2+} \rightarrow Fe^{2+} + HO_2^{\bullet} \quad (4)$$

Outras formas de redução de Fe^{3+} a Fe^{2+} ocorrem através das reações com $HO_2^{\bullet}$, radicais orgânicos ($R^{\bullet}$) e íons superóxido ($O_2^{\bullet -}$), conforme descrito pelas Equações 5, 6 e 7, respectivamente.

$$Fe^{3+} + HO_2^{\bullet} \rightarrow Fe^{2+} + O_2 + H^+ \quad (5)$$

$$Fe^{3+} + R^{\bullet} \rightarrow Fe^{2+} + R^+ \quad (6)$$

$$Fe^{3+} + O_2^{\bullet -} \rightarrow Fe^{2+} + O_2 \quad (7)$$

Dependendo da concentração de H_2O_2 no meio, este pode reagir com os radicais $^{\bullet}OH$ formando os radicais $HO_2^{\bullet}$ que ficam em equilíbrio com $O_2^{\bullet -}$ (Equações 8 e 9) (CHRISTENSEN; SEHESTED; CORFITZEN, 1982). As reações apresentadas pelas Equações 8 e 9 são consideradas as principais sequestradoras de H_2O_2, promovendo a sua destruição no meio, sendo consideradas reações parasitas no processo Fenton (BRILLAS; SIRÉS; OTURAN, 2009).

$$H_2O_2 + {}^{\bullet}OH \rightarrow H_2O + HO_2^{\bullet} \quad (8)$$

$$HO_2^{\bullet} \leftrightarrow H^+ + O_2^{\bullet -} \quad (9)$$

Os radicais $^{\bullet}OH$ podem atacar compostos orgânicos saturados (RH) ou aromáticos (ArH), gerando derivados desidrogenados e hidroxilados, conforme apresentado nas Equações 10 e 11, respectivamente (BUXTON et al., 1988). Os

radicais hidroxilados podem posteriormente reagir com O_2 formar radicais $HO_2^{\bullet}$ (Equação 12) (PIGNATELLO; OLIVEROS; MACKAY, 2006).

$$RH + {}^{\bullet}OH \rightarrow R^{\bullet} + H_2O \quad (10)$$

$$ArH + {}^{\bullet}OH \rightarrow ArHOH^{\bullet} \quad (11)$$

$$ArHOH^{\bullet} + O_2 \rightarrow ArOH + HO_2^{\bullet} \quad (12)$$

Além disso, ompostos orgânicos hidroxilados podem ser produzidos a partir de carbocátions (R^+) (Equação 13). Os radicais $R^{\bullet}$, além de auxiliarem na regeneração de F^{2+}, podem também promover a sua destruição, de acordo com a Equação 14, ou sofrer auto-dimerização (Equação 15) (BRILLAS; SIRÉS; OTURAN, 2009).

$$R^+ + H_2O \rightarrow ROH + H^+ \quad (13)$$

$$R^{\bullet} + Fe^{2+} + H^+ \rightarrow RH + Fe^{3+} \quad (14)$$

$$2R^{\bullet} \rightarrow R\text{-}R \quad (15)$$

Adicionalmente, dependendo das condições experimentais, uma série de reações parasitas podem afetar o processo Fenton, através da competição com o substrato orgânico pelo consumo de radicais, bem como pelo consumo de Fe^{2+} (Equações 16 a 23). (BIELSKI et al., 1985; CHRISTENSEN; SEHESTED; CORFITZEN, 1982; PIGNATELLO; OLIVEROS; MACKAY, 2006; RUSH; BIELSKI, 1985)

$$Fe^{2+} + {}^{\bullet}OH \rightarrow Fe^{3+} + OH^- \quad (16)$$

$$Fe^{2+} + HO_2^{\bullet} + H^+ \rightarrow Fe^{3+} + H_2O_2 \quad (17)$$

$$Fe^{2+} + O_2^{\bullet -} + 2H^+ \rightarrow Fe^{3+} + H_2O_2 \quad (18)$$

$$O_2^{\bullet -} + HO_2^{\bullet} + H^+ \rightarrow H_2O_2 + O_2 \quad (19)$$

$$HO_2^{\bullet} + HO_2^{\bullet} \rightarrow H_2O_2 + O_2 \quad (20)$$

$HO_2^{\bullet} + {}^{\bullet}OH \rightarrow H_2O + O_2$ (21)

$O_2^{\bullet -} + {}^{\bullet}OH \rightarrow OH^- + O_2$ (22)

${}^{\bullet}OH + {}^{\bullet}OH \rightarrow H_2O_2$ (23)

As Equações 8 e 16 são consideradas as principais reações indesejadas no processo Fenton devido ao seu significativo potencial de consumo de radicais $^{\bullet}OH$, reduzindo o poder oxidativo do sistema. Em alguns casos, a reação Fenton também pode ser afetada por íons inorgânicos sequestradores de radicais, tais como como cloreto, sulfato, nitrato, carbonato e bicarbonato (DE LAAT; TRUONG LE; LEGUBE, 2004).

Dentre as vantagens deste processo destacam se o custo relativamente baixo dos reagentes ferro e peróxido de hidrogênio (H_2O_2), a natureza ambientalmente segura dos reagentes, a simplicidade operacional (LOPEZ et al., 2004; PIGNATELLO; OLIVEROS; MACKAY, 2006).

2.3.2.2 Processo foto-Fenton

A adição de radiação UV pode trazer um acréscimo de eficiência à reação Fenton, pelo processo que é conhecido como foto-Fenton. A radiação utilizada pode ser de fontes artificiais, UVA ($315 < \lambda < 400$ nm), UVB ($285 < \lambda < 315$ nm), e UVC ($\lambda < 285$ nm), ou utilizando radiação solar ($\lambda > 300$ nm) (BRILLAS; SIRÉS; OTURAN, 2009; MALATO et al., 2007; OLLER et al., 2007).

Uma das limitações da reação Fenton é a acumulação de espécies de Fe^{3+} em solução, que desacelera o processo de tratamento. Com a aplicação de radiação na solução, ocorre fotorredução de complexos de hidróxido de ferro, tais como o $Fe(OH)^{2+}$, regenerando Fe^{2+} para a reação Fenton e produzindo radicais $^{\bullet}OH$ adicionais, conforme a Equação 24 (OLLER et al., 2007; PIGNATELLO, 1992). Além disso, a radiação UV também pode promover fotólise de complexos formados por Fe^{3+} e ligantes orgânicos, formando Fe^{2+} e espécies oxidantes fracas (Equação 25) (FAUST; ZEPP, 1993; ZUO; HOIGNE, 1992).

$$Fe(OH)^{2+} + h\nu \rightarrow Fe^{2+} + {}^{\bullet}OH \quad (24)$$

$$Fe^{3+}(L)_n + h\nu \rightarrow Fe^{2+}(L)_{n-1} + L^{\bullet}_{ox} \quad (25)$$

Em comprimentos de onda na região do ultravioleta C (UVC) também ocorre a fotólise de H_2O_2, gerando radicais $^{\bullet}OH$ e $HO_2^{\bullet}$ (Equações 27 e 28).

$$H_2O_2 + h\nu \rightarrow 2{}^{\bullet}OH \quad (27)$$

$$H_2O_2 + h\nu \rightarrow H^{\bullet} + HO_2^{\bullet} \quad (28)$$

O processo foto-Fenton possui uma eficiência mais elevada em valores de pH baixos (2,8 – 3,0), pois nestas condições a espécie de ferro dominante em solução é o $Fe(OH)^{2+}$, que é o complexo de hidróxido de ferro mais fotoativo (SUN; PIGNATELLO, 1993).

2.3.2.3 Processos eletro-oxidativos avançados

Processos eletro-oxidativos avançados (PEOAs) são uma das classes de POAs mais estudadas pela comunidade científica no tratamento de águas residuárias. Estes processos podem ser compostos de vários mecanismos individuais ou combinados, incluindo oxidação anódica, eletrogeração de H_2O_2, eletro-Fenton, FEF e eletrocoagulação (MOREIRA et al., 2017).

Nestes processos é aplicada uma corrente elétrica à solução através de eletrodos. A eletro-geração de H_2O_2 é um dos principais mecanismos de aumento do potencial oxidativo em PEOAs. Este mecanismo ocorre continuamente na superfície do cátodo, na presença de O_2, a partir da redução de dois elétrons, fornecendo H_2O_2 para a reação Fenton, conforme a Equação 29. Paralelamente, também ocorre a regeneração contínua de Fe^{2+} na superfície do cátodo, a partir da oxidação de Fe^{3+} (Equação 30) (BRILLAS; SIRÉS; OTURAN, 2009).

$$O_{2(g)} + 2H^+ + 2e^- \rightarrow H_2O_2 \quad (29)$$

$$Fe^{3+} + e^- \rightarrow Fe^{2+} \quad (30)$$

Em soluções alcalinas o O_2 presente no meio tende a se reduzir ao íon hidroperóxido (HO_2^-), a base conjugada do H_2O_2 (Equação 31) (BRILLAS; SIRÉS; OTURAN, 2009).

$$O_{2(g)} + H_2O + 2e^- \rightarrow HO_2^- + OH^- \quad (31)$$

A produção e estabilidade de H_2O_2 na solução depende de vários fatores, que incluem a configuração da célula eletrolítica, as propriedades do cátodo e as condições operacionais do sistema. Algumas reações parasitas podem ocorrer em sistemas de PEOAs, acarretando na perda de H_2O_2, por redução catódica e dissociação em solução, conforme apresentado pelas Equações 32 e 33, respectivamente (GALLEGOS; GARCÍA; ZAMUDIO, 2005).

$$H_2O_2 + 2H^+ + 2e^- \rightarrow 2H_2O \quad (32)$$

$$2H_2O_2 \rightarrow O_{2(g)} + 2H_2O \quad (33)$$

Duas diferentes configurações são geralmente aplicadas no PEOAs baseados na reação Fenton. Uma em que os reagentes Fe^{2+} e H_2O_2 são adicionados de fonte externa ao meio e os eletrodos são inertes, e outra em que apenas uma quantidade inicial de H_2O_2 é adicionada, e Fe^{2+} é fornecido por ânodos de sacrifício (ATMACA, 2009).

Paralelamente aos PEOAs, especialmente em valores de pH mais altos, nos quais a reação Fenton é menos eficiente, ocorre também o mecanismo de eletrocoagulação. Este mecanismo consiste na remoção de poluentes por meio da coagulação/floculação, seguida de precipitação, promovida por íons metálicos gerados no ânodo de sacrifício. A eletrocoagulação pode remover metais, partículas coloidais e compostos inorgânicos solúveis (MOLLAH et al., 2001).

Além disso, a oxidação anódica de poluentes é outro importante mecanismo dos PEOAs, podendo ocorrer por (i) transferência de elétrons na superfície do ânodo (M); (ii) espécies heterogêneas reativas de oxigênio produzidas como intermediárias da oxidação de água para oxigênio, incluindo $^{\bullet}OH$ fisiosorvido à superfície do ânodo ($M(^{\bullet}OH)$) (Equação 34), H_2O_2 e O_3 formados na superfície do ânodo (Equações 35 e

36); e (iii) outros oxidantes mais fracos produzidos em solução (PANIZZA; CERISOLA, 2009).

$$M + H_2O \rightarrow M(^{\bullet}OH) + H^+ + e^- \quad (34)$$

$$2M(^{\bullet}OH) \rightarrow 2MO + H_2O_2 \quad (35)$$

$$3H_2O \rightarrow O_3 + 6H^+ + 6e^- \quad (36)$$

A eficiência e seletividade da oxidação anódica de poluentes é influenciada significativamente pelo material dos eletrodos. Neste mecanismo pode ocorrer a degradação parcial dos poluentes, com formação de subprodutos refratários, ou a degradação completa, convertendo os poluentes em CO_2, água e íons inorgânicos (MOREIRA et al., 2017). Ânodos de BDD são descritos como os mais eficientes e menos seletivos para oxidação anódica, devido ao seu alto potencial de manter $^{\bullet}OH$ fisiosorvido à sua superfície sem a conversão em outros óxidos (MARSELLI et al., 2003; PANIZZA; CERISOLA, 2009).

Paralelamente, em processos eletroquímicos são formados agentes oxidantes indiretos a partir de compostos presentes no efluente, tais como cloreto, sulfato, fosfato e carbonato. Os principais agentes oxidantes indiretos formados são as espécies de cloro ativo Cl_2 e HClO, conforme apresentado nas Equações 37 e 38 (PANIZZA; CERISOLA, 2009).

$$2Cl^- \rightarrow Cl_2 + 2e^- \quad (37)$$

$$Cl_2 + H_2O \leftrightarrow HClO + Cl^- + H^+ \quad (38)$$

2.2.3 Parâmetros influentes nos POAs

Vários parâmetros podem influenciar a eficiência dos mecanismos de degradação dos POAs, tais como a carga orgânica inicial, concentração de reagentes, pH, O_2 dissolvido, material dos eletrodos, temperatura, complexantes, entre outros.

2.2.3.1 Carga orgânica inicial

Pesquisadores reportam que a taxa remoção de carga orgânica de efluentes por POAs tende a seguir uma cinética de pseudo-primeira ordem. Desta forma, quanto mais alta a concentração, maiores são as taxas de remoção, sendo atribuídas à rápida oxidação de compostos orgânicos por radicais $^{\bullet}OH$, em detrimento de reações parasitas (CAVALCANTI et al., 2013; HAMZA et al., 2009; MOREIRA et al., 2015a). No entanto, para concentrações muito elevadas de carga orgânica em processos de eletro-oxidação, autores observaram a diminuição do valor das constantes da cinética de pseudo-primeira ordem ou ainda a mudança para cinética de pseudo-ordem zero (EL-GHENYMY et al., 2013; GARCIA-SEGURA; BRILLAS, 2014; MOREIRA et al., 2015a). Estas mudanças são atribuídas ao fato de que a transferência de carga e massa entre eletrodos se tornam fatores limitantes, sendo reduzidas pela alta carga orgânica. Estes fatores podem aumentar a formação de complexos de Fe^{3+} com moléculas orgânicas, reduzindo a produção de $^{\bullet}OH$ (MOREIRA et al., 2017).

2.2.3.2 Concentração de reagentes Fenton

A concentração e fração de H_2O_2/Fe^{2+} é um fator que influencia de maneira significativa na eficiência de processos baseados na reação Fenton. Excesso ou insuficiência de um destes reagentes pode acarretar em reações de sequestro de $^{\bullet}OH$, pelas reações descritas nas Equações 8 e 16 (LOPEZ et al., 2004; UMAR; AZIZ; YUSOFF, 2010). Quantidades muito baixas de H_2O_2 acarretam na geração insuficiente de $^{\bullet}OH$ pra a oxidação da carga orgânica poluente. No entanto, o aumento da concentração de H_2O_2 para além de um valor limite, leva a redução de sua efetividade, além da formação de compostos orgânicos de difícil degradação (DENG; ENGLEHARDT, 2006). O excesso de Fe^{2+} em solução, por sua vez, além de competir com compostos orgânicos pelos radicais $^{\bullet}OH$, pode inibir a penetração de radiação UV no processo foto-Fenton devido à turbidez do meio (KIM; GEISSEN; VOGELPOHL, 1997; PÉREZ et al., 2002). As faixas de concentrações e frações ideais dos reagentes H_2O_2 e Fe^{2+} pode variar significativamente de acordo com a características do LAS a ser tratado, sendo parâmetros importantes de otimização em processos baseados na reação Fenton (UMAR; AZIZ; YUSOFF, 2010).

2.2.3.3 pH

O pH do meio é um dos principais fatores influentes na eficiência de PEOAs, afetando principalmente a especiação do ferro e solução e a estabilidade do H_2O_2 (BRILLAS; SIRÉS; OTURAN, 2009; ZHANG; CHOI; HUANG, 2005). Em geral, estudos reportam uma melhor eficiência destes processos quando utilizados valores de pH em faixas variando de 2 a 4 (MOREIRA et al., 2017). Valores de pH baixos estão associados a (i) produção de maiores quantidades de complexo Hidróxido-Fe(III) fotoativos em solução; (ii) redução/ausência da precipitação de ferro; (iii) ausência de carbonatos e bicarbonatos, que atuam como sequestradores de $^{\bullet}OH$; e (iv) não auto-decomposição de H_2O_2 em água e hidrogênio, que normalmente ocorre em valores de pH superiores a 5 (BUXTON et al., 1988; FAUST; ZEPP, 1993; MOREIRA et al., 2017; PIGNATELLO, 1992).

2.2.3.4 Intensidade/densidade de corrente e distância entre eletrodos

A intensidade ou de corrente é um parâmetro chave em PEOAs, estando diretamente associada a quantidade de espécies oxidantes produzidas. A corrente elétrica é responsável direta pela geração de M($^{\bullet}OH$) (Equação 34), promovendo a oxidação anódica da carga orgânica, além da produção de espécies de oxidação indireta tais como cloro ativo (Equações 37 e 38) (PANIZZA; CERISOLA, 2009). Além disso, nos processos baseados na reação Fenton, a corrente elétrica é responsável pela eletro-geração de H_2O_2 e regeneração de Fe^{2+} a partir de Fe^{3+}, conforme apresentado nas Equações 29 e 30 (MOREIRA et al., 2017).

De modo geral a taxa de remoção de poluentes aumenta com o aumento da corrente elétrica. No entanto, aumentos excessivos de corrente elétrica podem reduzir a sua eficiência devido a uma série de reações parasitas que tendem a ocorrer nestas condições, além de um elevado consumo energético e maior desgaste dos eletrodos (ANTONIN et al., 2015; FERNANDES et al., 2012; SIRÉS et al., 2014).

Menores distâncias entre eletrodos tendem a ter melhores eficiências na oxidação de poluentes, reduzindo a demanda de corrente elétrica e, consequentemente o consumo de energia. Isso ocorre, pois em menores distâncias,

através da condutividade do meio, existe uma menor resistência à passagem de corrente. Entretanto, distâncias muito baixas entre eletrodos podem reduzir a capacidade de vazão e reatores de fluxo (ATMACA, 2009; DÍEZ et al., 2016; ZHUO et al., 2020). Em geral, autores reportam o uso de distâncias entre eletrodos que variam de 0,5 a 3,0 cm (ATMACA, 2009; UMAR; AZIZ; YUSOFF, 2010).

2.2.3.5 Material dos eletrodos

Diversos materiais de eletrodos podem sem aplicados em PEOAs, e sua influência nos na eficiência de remoção de carga orgânica está relacionada com (i) as espécies liberadas em solução, especialmente ferro, (ii) o potencial de gerar $^{\bullet}OH$ fracamente fisiosorvido na superfície do ânodo, (iii) a capacidade de eletro-geração catódica de H_2O_2 e (iv) a durabilidade do material (BRILLAS; SIRÉS; OTURAN, 2009; GANIYU; ZHOU; MARTÍNEZ-HUITLE, 2018). Cátodos de grafite, carbono vítreo reticulado, fibra de carbono ativado, felt carbono e outros materiais de difusão de gás são comumente usados. Ânodos de grafite, platina, óxidos metálicos e BDD normalmente são preferidos (BRILLAS; SIRÉS; OTURAN, 2009; MOREIRA et al., 2017).

Dentre os ânodos estudados, destacam-se os de BDD, por sua alta durabilidade, robustez, eficiência, baixa seletividade, compatibilidade ambiental e baixa demanda de reagentes. Este tipo de ânodo é capaz de produzir altas quantidades de $^{\bullet}OH$ fracamente fisiosorvido em sua superfície, podendo degradar uma grande variedade de poluentes (FLOX et al., 2009; PANIZZA; CERISOLA, 2005; SIRÉS et al., 2008).

2.2.3.6 O_2 dissolvido

A partir da redução catódica do oxigênio em meio ácido e/ou neutro ocorre a eletro-geração de H_2O_2, conforme apresentado na Equação 29 (FOLLER; BOMBARD, 1995). Portanto, para que esse mecanismo seja favorecido, é necessário o fornecido oxigênio ou aeração contínua do reator, sendo que quanto maiores as taxas de oxigênio em solução, maior é a eletro-geração de H_2O_2. No entanto taxas muito altas de ar ou oxigênio podem causar problemas operacionais em alguns tipos de reatores,

tais como a redução da condutividade entre eletrodos e redução da vazão de efluente (MOREIRA et al., 2017).

2.3.4 Sistemas integrados de tratamento de LAS

A integração de POAS com oxidação biológica tem sido estudada por autores como alternativa de melhorar a relação custo-benefício do tratamento de LAS, aliando o baixo custo e simplicidade operacional de processos biológicos com a eficiência de degradação de bio-refratarios de POAS. Seibert et al. (2019b) investigaram a remoção de carga orgânica e toxicidade de LAS integrando um processo FEF com oxidação biológica aeróbia. Neste estudo foi constatada uma eficiência mais elevada do sistema quando aplicado um pré-tratamento FEF seguido de oxidação biológica, com remoção de contaminantes emergentes presentes no LAS bruto, com destaque para o Bisfenol A (BPA). Comportamento similar, de melhor eficiência do processo biológico quando precedido por um processo eletroquímico, foi observado por Pauli et al. (DE PAULI et al., 2018).

Diversos pesquisadores estudaram a aplicação destes processos de maneira integrada no tratamento de LAS. A Tabela 2 apresenta alguns destes estudos, com suas respectivas condições operacionais e eficiências na remoção de poluentes.

Tabela 2. Estudos de sistemas de POAS integrados com processos biológicos para o tratamento de LAS.

Processo de tratamento	Condições operacionais	Eficiência de remoção	Referência
Biofiltro e ozônio (recirculação)	Biofiltro: Condições aeróbias e anaeróbias. Um ciclo de 8 horas de tratamento. Ozônio: 1600 mg O_3 L^{-1}	DQO: 95,0% COD: 87,0%	(CASSANO et al., 2011)
Biofiltro e foto-Fenton como polimento final	Biofiltro: Condições aeróbias e anaeróbias. Um ciclo de 8 horas de tratamento.	DQO: 94,8% COD: 93,3%	

Processo de tratamento	Condições operacionais	Eficiência de remoção	Referência
	Foto-Fenton: 1190,5 mg H_2O_2 L^{-1}		
Biofiltro, ozônio e foto-Fenton como polimento final	Biofiltro: Condições aeróbias e anaeróbias. Um ciclo de 8 horas de tratamento. Ozônio: 1600 mg O_3 L^{-1} Foto-Fenton: 881 mg H_2O_2 L^{-1}	DQO: 95,0% COD: 95,3%	
TiO_2/UV acoplado tratamento biológico com lodo ativado	Processo biológico: condições aeróbias, 500 horas TiO_2/UV: pH 5	DQO: 94,0% DBO: 90,0%	(CHEMLAL et al., 2014)
Foto-Fenton solar combinado com reator aeróbio de biomassa imobilizada	Foto-Fenton: 60 mg Fe^{2+} L^{-1}, energia acumulada de 100 kJ_{UV}, 3.0 mmol H_2O_2 kJ_{UV}^{-1}	DBO: 100% DQO: 95,0% COD: 92,4%	(VILAR et al., 2011)
Eletro-Fenton combiado com reator biológico de aterro envelhecido	Biológico: condições aeróbias e anaeróbias Eletro-Fenton: cátodo de difusão de gás e ânodo de Ti/PbO_2; 3 cm de espaço entre eletrodos; 30 cm de área útil por eletrodo; 120 min de eletrólise	DQO: 98,5%, DBO: 99,9% COT: 98,0%	(LEI et al., 2007)
Foto-eletro-Fenton seguido de oxidação biológica	Biológico: condições aeróbias, 24 horas de processo Foto-eletro-Fenton: eletrodos de ferro; adição inicial de 9000 mg H_2O_2 L^{-1} e 60 mg Fe^{2+} L^{-1}; intensidade de	DQO: 72,6% DBO: 53,4% Carbono Total (CT): 91.9% Abs. 254 nm: 91.6%	(SEIBERT et al., 2019b)

Processo de tratamento	Condições operacionais	Eficiência de remoção	Referência
	correte 2.3 A; pH 3,5-4,5; 45 min de processo.		
Eletrocoagulação seguida de oxidação biológica	Biológico: condições aeróbias Eletrocoagulação: densidade de corrente de 128,57 A m^{-2}; pH 5; 120 min de eletrólise.	DQO: 89,0% COD: 95,0%	(DE PAULI et al., 2018)
Arraste de ar, processo Fenton, tratamento biológico e coagulação.	Arraste de ar: taxa de ar de 15 L min^{-1}, pH 11, tempo de 18 h; processo Fenton: pH 3,0, 4 g Fe L^{-1}, 6 g H_2O_2 L^{-1}. Tratamento biológico: reator de batelada sequencial, ciclo de 24 h, pH 7. Coagulação com [Fe2(SO4)3]: 223 mg Fe L^{-1}, pH 5.	DQO: 93,3% DBO: 84,5%	(GUO et al., 2010)
Tratamento biológico anaeróbio por oxidação de amônio seguido de foto-Fenton com UVC	Biológico: ciclo de 24 h, pH 7,4. Foto-Fenton: pH 3, 150 mg Fe L^{-1}, 1 g H_2O_2 L^{-1}	DQO: 98% DBO: 100%	(ANFRUNS et al., 2013)
Tratamento biológico anaeróbio seguido de foto-Fenton solar seguido de tratamento biológico aeróbio.	Biológico anaeróbio: ciclo de 58 dias, pH 7,5 – 9,0, oxigênio dissolvido. Foto-Fenton solar: pH 2,8, 80 mg Fe L^{-1}, 100-500 mg H_2O_2 L^{-1}. Biológico aeróbio: 29 dias de tratamento, pH 7,5 – 9,0.	DQO: 98,4% DBO: 99,1% COD: 98,2%	(SILVA et al., 2013)
Processo Fenton + Tratamento Biológico e reator de aeróbico de	Processo Fenton: pH 3, 1,1 Fe g L^{-1}; 2 g H_2O_2 L^{-1}.	DQO: 98,6%	(ZHANG et al., 2013)

Processo de tratamento	Condições operacionais	Eficiência de remoção	Referência
membrana submersa + Osmose reversa	Processo biológico: membrana; taxa 0,1 – 0,15 m^3 ar h^{-1}; fluxo líquido de 2 L m^2 h^{-1}. Osmose reversa: 66 cm^2 de área filtrante; pressão de 2,8 MPa.		
Tratamento biológico aeróbio + coagulação + foto-eletro-Fenton solar + tratamento biológico anaeróbio	Tratamento biológico aeróbio: teste de Zhan-Wellens; ciclo de 138 – 164 h; pH 6,5 – 9,0; 2 – 4 mg O_2 L^{-1}. Coagulação com $FeCl_3$: 240 mg Fe L^{-1}, pH 3,3. Foto-eletro-Fenton solar: pH 2,8; 60 mg Fe L-1; densidade de corrente de 200 mA cm^{-2} Tratamento biológico anaeróbio: teste de Zhan-Wellens	DQO: 97%	(MOREIRA et al., 2015b)

2.4 ENSAIOS DE TOXICIDADE

Ensaios de ecotoxicidade são definidos pela resolução CONAMA 430 de 2011 como métodos para detectar e avaliar a capacidade de agentes tóxicos capazes de provocarem efeitos noviços, usando bioindicadores de grandes grupos da cadeia ecológica (BRASIL, 2011). Os ensaios biológicos de ecotoxicidade são ferramentas de diagnóstico adaptadas para determinar o efeito de agentes físico/químicos sobre organismos testes, sob condições experimentais controladas. Estes efeitos podem ser de inibição ou ampliação, causando reações nos organismos como morte, crescimento, proliferação, multiplicação, alterações morfológicas, fisiológicas ou histológicas (SOBRERO; RONCO, 2004).

Pesquisadores têm realizado estudos de toxicidade em LAS utilizando os bioindicadores *Hordeum Vulgare* (SANG; LI; XIN, 2006); *Rasbora sumatrana*, *Macrobrachium lanchesteri* e *Lycoperson esculentum* (BUDI et al., 2016); *Daphnia magna* (MAIA et al., 2015); *Lactuca sativa* (BORBA et al., 2019; DE PAULI et al., 2017; WELTER

et al., 2018); *Artemia salina* (DE PAULI et al., 2017), *Eruca sativa* e *Allium cepa* (KLAUCK; RODRIGUES; SILVA, 2015).

3 LANDFILL LEACHATE TREATMENT BY A BORON-DOPED DIAMOND-BASED PHOTO-ELECTRO-FENTON SYSTEM INTEGRATED WITH BIOLOGICAL OXIDATION: A TOXICITY, GENOTOXICITY AND BYPRODUCTS ASSESSMENT

Nota: Os resultados deste estudo estão apresentados na forma de um artigo científico na seção 3.

Leandro Pellenz[1]♣, Fernando H. Borba[1], Daniel J. Daroit[1], Manoel F. M. Lassen[1], Suzymeire Baroni[1], Camila F. Zorzo[1], Raíssa Engroff Guimarães[1], Fernando R. Espinoza-Quiñones[2], Daiana Seibert[3]

[1] Postgraduate Program of Environment and Sustainable Technologies, Federal University of Fronteira Sul, Av. Jacob Reinaldo Haupenthal, 1580, 97900-000, Cerro Largo, RS, Brazil

[2] Postgraduate Program of Chemical Engineering, West Paraná State University, Rua da Faculdade 645, Jd. Santa Maria, 85903-000, Toledo, PR, Brazil.

[3] Postgraduate Program of Chemical Engineering, State University of Maringa, UEM, Av. Colombo, 5790, Maringa, Parana, CEP: 87020-900, Brazil.

[*] Corresponding author.

Email address: leandropelenz@hotmail.com (L. Pellenz).

Permanent address: Federal University of Fronteira Sul-UFFS, Rua Jacob Reinaldo Haupenthal, 1580, Sala 104, Bloco dos Professores. Bairro Industrial, 97900-000, Cerro Largo, RS, Brazil.

HIGHLIGHTS

- A new configuration of a PEF reactor was proposed and studied.
- BDD and soft iron anodes were compared.
- Intermediary byproducts were identified in (un) treated LL.
- PEF was integrated with BO
- Reduction of phytotoxicity, genotoxicity and LL purification.

GRAPHICAL ABSTRACT

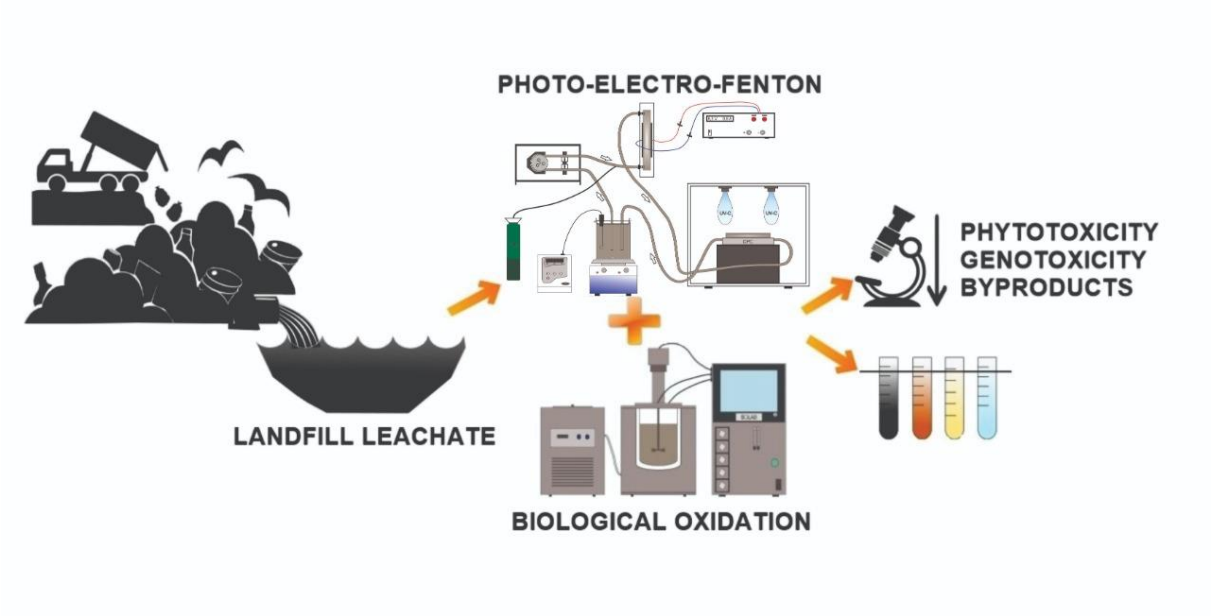

ABSTRACT

A photo-electro-Fenton (PEF) reactor employing boron-doped diamond (BDD) and soft iron anodes was studied in landfill leachate (LL) treatment. The reactor operation parameters (ROP) H_2O_2 concentration, current intensity and flow rate were investigated in the removal of Abs 254 nm. The PEF process with BDD anode, operating at the best operational conditions, was used as a pre-treatment and enabled biological oxidation (BO). The treatment strategy of PEF followed by BO showed to be the most efficient, reaching reductions of 77.9% chemical oxygen demand (COD), 71.5% total carbon (TC) and 76.3% radiation absorbance in 254 nm (Abs 254 nm), as well as a significant reduction in the genotoxicity (Allium cepa), observed by an increase in the mitotic index (MI) (131.5%) and decrease in the abnormalities (47.8%). The reduction of the toxic potential of LL using the integration of processes was also observed in the gas chromatography-mass spectrometry (GC-MS) byproducts analysis, which indicated the removal of emerging contaminants, such as Bisphenol-A (BPA), N,N-Diethyl-3-methylbenzamide (DEET) and Diisooctyl phthalate (DIOP). Thus, the PEF process integrated with BO presented a considerable efficiency in the removal of contaminants present in LL, becoming an alternative for the minimization of the environmental impacts caused by the discharge of this effluent in the environment.

Keywords: Photo-electro-Fenton, BDD, biological oxidation, landfill leachate, toxicity.

RESUMO

Um reator foto-eletro-Fenton (FEF) utilizando eletrodos de diamante dopado com boro (BDD) e ferro doce foi estudado no tratamento de lixiviado de aterro sanitário (LAS). Os parâmetros operacionais do reator (ROP) concentração de H_2O_2, intensidade de corrente e vazão foram investigados na remoção de absorbância de radiação em 254 nm (Abs 254 nm). O processo FEF, operando nas melhores condições operacionais, foi utilizado como pré-tratamento e possibilitou a oxidação biológica (OB). A estratégia de tratamento PEF seguida de OB demonstrou ser a mais eficiente, atingindo reduções 77,9% de demanda química de oxigênio (DQO), 71,5% de carbono total (TC) e 76,3% de Abs 254 nm, bem como significativa redução na genotoxicidade (*Allium cepa*), observada por um aumento no índice mitótico (MI) (131,5%) e uma diminuição nas anormalidades (47,8%). A redução do potencial tóxico de LAS utilizando a integração de processos também foi observada na análise de subprodutos por cromatografia gasosa-espectrometria de massas (CG-EM), que indicou a remoção de contaminantes emergentes, tais como Bisfenol-A (BPA), N,N-dietil-3-metilbenzamida (DEET) e Diisooctil ftalato (DIOP). Desta forma, o processo FEF integrado com OB apresentou uma eficiência considerável na remoção de contaminantes presentes em LAS, se tornando uma alternativa para a minimização dos impactos ambientais causados pelo descarte deste efluente no meio ambiente.

Keywords: Foto-eletro-Fenton, BDD, oxidação biológica, lixiviado de aterro sanitário, toxicidade.

3.1 INTRODUCTION

Most of the human activities generate some kind of waste. Due to factors such as urbanization, technological evolution and population growth, municipal solid waste has become one of the most relevant waste classes, with increasing generation rates and a varied composition (DAS et al., 2019; KAZA et al., 2018). With a good cost-effectiveness relationship, landfills are the most applied alternatives for final disposal of municipal solid waste around the world. In landfills, the solid waste decomposes by physical, chemical and biological processes, generating, among other byproducts, significant amounts of LL (DAS et al., 2019; RENOU et al., 2008).

LL is an effluent with a high pollution potential, containing a large and complex variety of organic and inorganic pollutants, including aromatic hydrocarbons, humic and fulvic acids, esters, alcohols, amides, ammonia nitrogen, heavy metals, among others (GUPTA et al., 2014; NAVEEN et al., 2017; ÖMAN; JUNESTEDT, 2008). Because of its composition, if improperly managed, LL can cause serious damage to the environment and to human health, highlighting its toxic, mutagenic, genotoxic and estrogenic effects (BADERNA; CALONI; BENFENATI, 2018).

Some processes, such as microfiltration, ultrafiltration, nanofiltration and reverse osmosis are able to efficiently remove the pollutant load from LL using membranes systems. However, these techniques do not degrade the pollutants, only concentrate on a smaller volume, still leaving an environmental liability to be solved (NAVEEN et al., 2017; RENOU et al., 2008). Furthermore, the recalcitrant and toxic characteristics of the pollutants contained in LL usually limit the efficiency and applicability of low cost conventional degradation methods, such as biological oxidation (RENOU et al., 2008). Thus, advanced treatment processes that are able to degrade and/or mineralize the contaminants become an important pre-treatment alternative for reduction of toxicity and recalcitrance of LL (SEIBERT et al., 2019b).

Within this context, due to its high efficiency and low selectivity in degradation of compounds in solution, the electrochemical advanced oxidation processes (EAOPs) based in the production of hydroxyl radicals ($^{\bullet}OH$) become an interesting alternative for studies. These processes have as central mechanism the Fenton reaction, that can be assisted by photo and electro oxidation, increasing the radicals production rate, and

consequently, the efficiency of pollutants degradation (BRILLAS; SIRÉS; OTURAN, 2009; MOREIRA et al., 2017).

Several electrode materials have been applied in the electric current supply for EAOPs in the treatment of LL, such as iron (ATMACA, 2009; SEIBERT et al., 2019b), graphite (SRUTHI et al., 2018), RuO_2/Ti – Ti (XIAO et al., 2013), Ti/PbO_2 (LEI et al., 2007), Ti/RuO_2/IrO_2 – stainless steel (ZHANG et al., 2011), TiO_2/Ti – graphite (BAIJU et al., 2018), and boron-doped diamond (BDD) (YAZICI GUVENC; DINCER; VARANK, 2019; ZOLFAGHARI et al., 2016). Comparative studies indicate that BDD anodes are the most effective in the mineralization of pollutants due to its durability, robustness, efficiency, low selectivity, environmental compatibility and low reagents demand (FLOX et al., 2009; PANIZZA; CERISOLA, 2005; SIRÉS et al., 2008). These anodes produce high amounts of $^{\bullet}OH$ weakly absorbed on its surface, which promote the degradation of several types of pollutants, such as carboxylic acids (OCHIAI et al., 2011), dyes (PANIZZA; CERISOLA, 2008; PEREIRA et al., 2016; RAMÍREZ et al., 2013), cyanides (CAÑIZARES et al., 2005), surfactants (LOUHICHI et al., 2008), pesticides (ALVES et al., 2013; CAI et al., 2020; ZHUO et al., 2020), pharmaceuticals (BRINZILA et al., 2012; DA SILVA et al., 2019a, 2019b), among others.

Despite a significant degradation of pollutants present in LL, some byproducts formed in the EAOPs may remain in the effluent. Aiming to increase the effectiveness of the treatment, researchers have investigated the application of multistage techniques, integrating biological with physical-chemical oxidation processes (BAIJU et al., 2018; DE MORAIS; ZAMORA, 2005; DE PAULI et al., 2018; INGLEZAKIS et al., 2018; MOROZESK et al., 2017; SEIBERT et al., 2019b).

This research assessed the PEF process in the treatment of LL in a batch recirculation system, making a comparison between a system using soft iron electrodes and one with BDD anode and soft iron cathode. The best conditions H_2O_2 concentration, current intensity and flow rate of the system were identified. Abs 254 nm, COD, TC, as well as phytotoxicity to the bioindicator *Lactuca sativa*, genotoxicity in *Allium cepa* and GC-MS byproducts analyses were used as parameters to evaluate the efficiency of the process and to compare the different investigated systems. Additionally, an activated sludge BO process was integrated to the PEF process, aiming to increase the efficiency in the removal of the organic load and to improve the

cost-effectiveness of the system. Likewise, the removals of COD, TC, phytotoxicity and genotoxicity, as well as the process byproducts were assessed for the integrated system. The study of these techniques in preliminary separated lab scale reactors is an important stage to enable real scale integrated applications in the treatment of LL.

Thus, this research presents a novel approach where a well know PEF system – soft iron electrodes – was compared with a with system using BDD anodes. The BDD anode-based PEF process, applied as pre-treatment, reduced the toxicity of the LL, enabling the application of an activated sludge BO technique. In order to better assess the studied techniques, a broad analysis of the treated samples was carried out, including Abs 254 nm, COD, TC, phytotoxicity (*Lactuca sativa*), genotoxicity (*Allium cepa*), byproducts (GC-MS) and metal elements (Total reflection X-rays fluorescence – TXRF).

3.2 MATERIALS AND METHODS

3.2.1 Samples, reagents, solvents and analytical determinations

The LL samples were collected in a sanitary landfill of a waste processing plant located in the northwest region of Rio Grande do Sul – Brazil and stored according to the Standard Methods (RICE; PUBLIC HEALTH ASSOCIATION, 2012). Hydrogen peroxide (ALPHATEC, 35%) and O_2 (White Martins, 99.5%) were used in the PEF reactions. Sulfuric acid (Vetec, 1.5 M) and sodium hydroxide (ALPHATEC, 6 M) were applied in the solution pH adjustment. Ultrapure water used in the phytotoxicity and genotoxicity assays was produced by a Millipore Direct-Ultrapure water system (MilliQ®). Pesticide free *L. sativa* seeds and *A. cepa* bulbs were used in the phytotoxicity and genotoxicity assays, respectively. The activated sludge used as inoculum for the BO tests was provided by a dairy industry located in the western region of Paraná state – Brazil, and preserved under aeration. The determinations of pH, Abs 254 nm TC/TN, conductivity and turbidity were carried out using the equipment pHmeter (MS-Tecnopon, mPA-210), spectrophotometer (Thermo-Scientific, Evolution 201), TOC analyzer (Shimadzu, TOC-L series), conductivity meter (Digimed DM-32) and turbidimeter (PoliControl, AP 2000 iR), respectively. The H_2O_2 concentration was measured using by spectrophotometry, using the ammonium metavanadate method, describe by Nogueira et al. (NOGUEIRA; OLIVEIRA; PATERLINI, 2005). Color was

determined applying the Platinum-cobalt (Pt-Co) method, BOD5 measured by manometric respirometry, following the OECD-301F protocol – OxiTop, and COD was determined by the closed reflux colorimetric method (RICE; PUBLIC HEALTH ASSOCIATION, 2012). Metal elements were measured by total reflection X-rays fluorescence (Bruker, S2 PICOFOX).

Genotoxicity, phytotoxicity and GC-MS analysis were carried out according to methodologies described by Fiskesjö (1993), Sobrero and Ronco (2004), and Seibert et al. (2019a)(FISKESJÖ, 1993; SEIBERT et al., 2019b; SOBRERO; RONCO, 2004), respectively. The methodologies described in details are presented in the Supplementary Material.

3.2.2 Photo-electro-Fenton reactor and experimental procedure

A bench scale reactor was built to perform the Fenton process assisted by photo and electro degradation (Fig 1SM). The reservoir of the reactor was composed of a 1000-mL borosilicate beaker, a pHmeter (MS-Tecnopon, mPA-210) and a magnetic stirrer (Cienlab, CE-1540/QA-18) for homogenization of the effluent. An electrolytic cell was built for the electro oxidation process using acrylic plates externally and soft iron electrodes with a 1-cm gap between cathode and anode. The cell was positioned in vertical direction and its electrodes were connected to an electric power supply (BK Precision - 1685B) with intensity control. A wooden chamber internally coated with stainless steel (50.4 cm x 62.0 cm x 43.0 cm) and a compound parabolic collector were used for the photo-Fenton process. The UVC radiation was provided by two UV-C lamps (13 W, Philips TUV PL-S), which emit radiation with a maximum intensity peak around 254 nm wavelength and an integrated intensity of 0.3 W m^{-2}, determined by a broadband radiometer (Apogee, UM-200).

The operation was conducted by circulating the LL in a cycle using a peristaltic pump (MS-Tecnopon, LDP-201-3) with flow rate control. Using a hose system, the effluent was first pumped through the electrolytic cell, upwardly, in order to completely fill the gap between the electrodes. O_2 was injected in the system at a rate of 0.2 L min^{-1}. In sequence, the LL was pumped to the UVC chamber, passing inside compound parabolic collector, through a glass tube placed in horizontal direction, and ending the cycle, the effluent returned to the reservoir (Fig. 1SM). The concentration of H_2O_2 was

monitored and kept constant by repositions according to conditions defined in the experimental design. The repositions were made in the circulation hose, after the electrolytic cell, in order to reduce the degradation of H_2O_2 in the system.

1000 mL of raw LL was used to perform the experimental runs. First, a pH adjustment (4-5) was made, followed by the addition of pre-determined concentrations of H_2O_2. O_2 was injected in the system, at the entrance of the electrolytic cell, in order to enhance the H_2O_2 electro generation (MARTÍNEZ-HUITLE; FERRO, 2006). The H_2O_2 concentration, current intensity and flow rate of each experiment were set according to the experimental design. With the PEF system in operation, samples were collected in process times 0, 5, 15, 30, 45 and 60 min for measurement of radiation absorbance in 254 nm wavelength (Abs 254 nm), COD and TC. Also, samples were collected in times 0; 7.5; 15; 22.5; 30; 38.5; 45; 52.5; and 60 min, to monitor and add H_2O_2 when necessary.

3.2.3 Biological oxidation reactor and experimental procedure

Activated sludge BO systems integrated to physicochemical processes have been investigated by researchers as a simple and low cost techniques of organic load reduction in LL (DE PAULI et al., 2018; KURNIAWAN et al., 2010; SEIBERT et al., 2019b).

A bioreactor (SOLAB, SL-135), made of a 5-L jacketed cylindrical recipient, coupled to a thermostatic bath, for temperature control, was used for the BO process (Fig 1SM). The reactor was equipped with pH and O_2 monitoring probes, coupled to a computer that automatically controlled these parameters by adding H_2SO_4 or NaOH, and by sparging sterile air and stirring the solution, respectively.

A volume of 3 liters of LL plus 300 mL of inoculum (activated sludge from a dairy effluent aerobic lagoon) was used at each experimental batch. The system was aerated at a rate of 2 L air min^{-1} and stirred at 50 to 500 RPM, according to the measured oxygen concentration (minimum 50% of O_2 measured in atmosphere). The pH of the solution was held between 6.5 and 7.5. Each experimental batch was carried out for 72 hours, with collection of aliquots every 2 hours, for COD, TC and optical density (OD) determination. OD, which is related to bacterial growth, was measured

using a spectrophotometer at 593 nm. The wavelength used for OD measurements was defined by scan.

3.3 RESULTS AND DISCUSSION

3.3.1 Landfill leachate characterization

The physical-chemical characteristics of the raw and treated LL samples are presented in Table 1.

Table 1. Characterization of the treated and untreated LL samples.

Parameter	Raw LL	Treated LL			
		PEF	BO	PEF + BO	BO + PEF
Abs 254 nm (a.u.) (dil 1:25)	1.343 ± 0.08	0.611 ± 0.06	1.337 ± 0.08	0.318 ± 0.05	0.781 ± 0.06
Color (mg Pt-Co L^{-1}) Dil. 1:10	1374.4 ± 56	314.6 ± 14	1352.9 ± 61	155.4 ± 9	493.8±19
TC (mg C L^{-1})	4732.1 ± 11	2873.2 ± 82	4562.8 ± 105	1352.1 ± 80	852.1 ± 83
TN (mg N L^{-1})	1008 ± 76	852 ± 55	1190 ± 73	731 ± 56	976± 79
BOD_5 (mg O_2 L^{-1})	1592.5 ± 47	1340.1 ± 39	1583.1 ± 51	398.3 ± 21	1241.6 ± 39
COD (mg O_2 L^{-1})	6924.0 ± 95	3621.8 ± 82	6841.3 ± 97	1531.9 ± 73	4491.5 ± 77
BOD_5/COD	0.23	0.37	0.23	0.26	0.28
Conductivity (µS cm^{-1})	23.2 ± 1	31.5 ± 1	23.1 ± 1	29.3 ± 1	31.5 ± 1
Turbidity (NTU)	102.3 ± 4	35.4 ± 4	96.5 ± 4	22.4 ± 3	43.2 ± 4
pH (Sörensen scale)	7.8 ± 0.3	4.4 ± 0.2	7.0 ± 0.2	7.0 ± 0.2	4.5 ± 0.2

The presence of organic compounds is evidenced by the high BOD_5, COD and TC values, as well as Abs 254 wavelength absorbance, which is related aromatic substances present in the LL, mainly humic and fulvic compounds (DENG et al., 2018). The dark brown color of the LL is also attributed to the presence of humic compounds

(SILVA et al., 2016). The alkaline pH value, high conductivity and total dissolved solids values can be related to the presence of cations and anions such as potassium, sodium, chloride, nitrate, sulfate, ammonia, coming from biochemical decomposition of waste and dissolution process that occurs in the landfill sites (NAVEEN et al., 2017). In addition the low BOD_5/COD ratio indicate that a single BO process may not be the most suitable treatment strategy for LL, since its composition may limit and/or inhibit the microbial activity (BAIJU et al., 2018).

A raw LL sample was analyzed by GC-MS (see Table 2SM). 14 compounds were detected: Diethylene glycol diethyl ether (Diethyl carbitol); 2-butoxyacetic acid; 3,5,5-trimethylhexanoic acid; 2-(5-ethenyl-5-methyloxolan-2-yl)propan-2-ol (Linalyl oxide); (1R,2S,3S)-1,2-dimethyl-3-prop-1-en-2-ylcyclopentan-1-ol (Plinol C); (4S)-4-(2-hydroxypropan-2-yl)cyclohexene-1-carboxylic acid (Oleuropeic acid); DIOP; DEET; 2,6-Dimethoxybenzoic acid (DBA); benzyl decanoate; 1-Hexacosene; 10-methylnonadecane; BPA and tetracosane; in retention times (RT) 4.19, 4.27, 4.43, 4.70, 4.86, 4.91, 5.29, 5.88, 6.0, 6.25, 9.81, 10.09, 11.53 and 11.99 min, respectively. Among these compounds Diethylene glycol diethyl ether, DIOP, DEET, DBA and BPA are listed by EPA (USEPA, 2012) as potential endocrine disrupting chemicals (EDCs). According to Seibert et al. (SEIBERT et al., 2019a), BPA is the most detected EDC in LL over the world and its presence in landfill sites is mainly related to materials such as plastic, polycarbonates and epoxy resins. BPA is associated with several adverse health effects, including cancer incidence, reproductive problems, anxiety and depression (BADERNA; CALONI; BENFENATI, 2018; CANLE; FERNÁNDEZ PÉREZ; SANTABALLA, 2017). DIOP is used in plasticizers of rubber and vinyl, cellulosic and acrylate resins (HSDB, 2019). Phthalates in general are related to adverse reproductive effects (BAKEN et al., 2019). DEET is widely used as an insect repellent (KAPELEWSKA; KOTOWSKA; WIŚNIEWSKA, 2016) and according to Sui et al. (SUI et al., 2010), it does not have good removal rates by conventional wastewater treatments. To date, DBA, has not been reported as toxic in the literature.

3.3.2 PEF preliminary tests

Preliminary tests of the PEF system employing soft iron electrodes were performed with an initial addition of 1000 mg H_2O_2 L^{-1} and no reposition during the

process. The influence of UVC radiation and current intensity in the consumption of H_2O_2 and removal of Abs 254 nm were monitored (see Fig. 2SM).

The system with the absence of UVC radiation and current intensity was not able to significantly degrade pollutants present in LL, possibly because low amounts of $^{\bullet}OH$ were produced by Fenton reaction, reaching only 7% of Abs 254 nm removal in 30 min. This was also evidenced by the low consumption of H_2O_2, possibly reducing the $^{\bullet}OH$ production under these conditions. When UVC + H_2O_2 was applied, the treatment removed approximately 33% of Abs 254 nm in 30 min, consuming 160 mg H_2O_2 L^{-1}. This can be associated with the photolysis of H_2O_2 molecule by UVC radiation, producing small amounts of $^{\bullet}OH$, which partially removed aromatic compounds present in LL. The LL treatment applying UVC + H_2O_2 + current intensity (0.5 A) showed to be the best condition, probably due to the iron species released in solution by the electrodes, promoting the Fenton reaction and thus increasing the $^{\bullet}OH$ production. As a result, 54% of Abs 254 nm was removed in 30 min of process, with the consumption of 700 mg H_2O_2 L^{-1} (see Fig. 2SM).

In subsequent tests, the Abs 254 nm and COD reduction were monitored for different operational conditions, including O_2 flow rate into the system (0.2 L min^{-1}), UVC radiation, H_2O_2 concentration (1000 mg L^{-1} constant, with repositions) and current intensity (0.5 A). The best efficiency of the process was achieved when all these conditions were applied, reaching removals 80% Abs 254 nm and 82 % COD, in 120 min of process (see Fig. 3SM).

The use of an electric current intensity is beneficial for the PEF process efficiency, since H_2O_2 is produced in situ, on the surface of the cathode (BRILLAS; SIRÉS; OTURAN, 2009; NIDHEESH; GANDHIMATHI, 2012). Even with external addition of H_2O_2, the experimental run without use of current intensity did not present good removal rates. Under these conditions the COD and Abs 254 nm were reduced 45%, in 120 min of process (see Fig. 3SM). This fact can be related to the low iron concentration in solution, which was not release from the electrode with no current. The low iron concentration in solution impairs the Fenton reaction, thus implying in lower $^{\bullet}OH$ production by H_2O_2 and Fe^{2+} reaction (KHATRI; SINGH; GARG, 2018). On the other hand, when no H_2O_2 was added and current intensity was employed, the COD and Abs 254 nm removals increased compared to the previous condition (64%

for both parameters), ascribed to the in situ H_2O_2 generation and the release of iron species in solution, which participate of the Fenton reaction (see Fig. 3SM). The application of UVC radiation to the solution promotes photolysis of iron complexes as well as extra $^{\bullet}OH$ production by the H_2O_2 cleavage (BENITO et al., 2017; LIU et al., 2018). The absence of UVC in the process decreased its efficiency, reaching removal rates of 64% and 60%, in 120 min, for COD and Abs 254 nm, respectively. Among the investigated parameters, the addition of dissolved O_2 showed to be the less influent on the process efficiency. When no O_2 was added the efficiency slightly decreased – 73% COD and 69% Abs 254 nm removal – compared to the experimental run in which all parameters were applied (see Fig. 3SM). During electro-oxidative processes, the presence of oxygen is also related to the increase of H_2O_2 electro-generation (WANG et al., 2010).

Considering the parameters that most affect the process efficiency, especially the addition of H_2O_2 and electric current intensity, preliminary tests varying the values of these parameters, as well as the flow rate of the system, were carried out as showed in Figure 4SM. Regarding the applied current intensity, too high values may promote side reactions such as O_2 reduction to H_2O and H_2O_2 oxidation at the surface of the anode. On the other hand, too low electric current intensity can impair the H_2O_2 electro-generation (BENITO et al., 2017; BRILLAS; SIRÉS; OTURAN, 2009; DIVYAPRIYA; NAMBI; SENTHILNATHAN, 2018; FLOX et al., 2009; KHATRI; SINGH; GARG, 2018). Thus, the experimental run with higher current intensity (0.5 A) combined with a lower H_2O_2 concentration (500 mg L^{-1}) provided better removal rates of COD (84%) and Abs 254 nm (83%) in 120 min of process when compared to the application of 0.2 A current intensity and 1000 mg H_2O_2 L^{-1} (57% of COD removal and 59% of Abs 254 nm removal) (see Fig. 4SM). It is reported in literature that an optimal amount of H2O2 should be employed in Fenton based processes due to fact that high concentrations promote undesired reactions such as $^{\bullet}OH$ scavenging, and low concentrations may not be enough to produce the required $^{\bullet}OH$ to oxidize the organic load (BRILLAS; SIRÉS; OTURAN, 2009; MOREIRA et al., 2017; XU; WANG, 2011).

Regarding the reactor flow rate, high flows may not provide the suitable reaction time aiming to oxidize the pollutants at the anode's surface, since in this case the retention time will be lower. On the other hand, low flows can create bypass and may

provide low solution homogenization. The experimental run in which 0.8 L min^{-1} flow rate was used showed to be slightly more efficient than the experiment with 0.2 L min-1 (see Fig. 3SM).

3.3.3 Response surface methodology (RSM)

The best performance of the PEF process in the degradation of pollutants present in LL was determined by a central composite rotational design (CCRD), based on a response surface methodology, described by Seibert et al. (2019a). At fixed experimental conditions of 0.2 L O_2 min^{-1} and controlled pH between 4 and 5, using iron anode, 17 experimental runs were carried out (8 factorial points, 6 axial points and 3 replicates at the central point), investigating the ROP H_2O_2 concentration (27.3 – 1372.7 mg L^{-1}), current intensity (0.36 – 1.04 A), and flow rate of the system (0.06 – 0.74 L min^{-1}). The removal of Abs 254 nm (%) was used as response variable (see Table 1SM).

A substantial decrease in the Abs 254 nm (69.5%) was observed in 15 min of PEF process, applying 300 mg H_2O_2 L^{-1}, 0.9 A current intensity, and flow rate of 0.6 L min^{-1} (see Table 1SM). The influence of the ROP (q_1, q_2 and q_3) in the removal of Abs 254 nm was expressed by a polynomial quadratic model (see Equation 1) with confidence interval of 95% (p-value < 0.05). The analysis of variance (ANOVA) validated the proposed mathematical model, presenting F_{calc} (4.52) > F_{tab} (3.22).

$$R = a_0 + \sum_{i=1}^{n} a_i q_i + \sum_{i=1}^{n} \sum_{j \neq 1}^{n} a_{ij}\, q_i q_j \qquad (1)$$

Where R is the response variable, q_i and q_j are the operation parameters, a_0, a_i and a_{ij} are the adjusted coefficients and n is the number of parameters.

3D response surfaces allowed to verify that the best Abs 254 nm removal performance, in 15 min of process, varied from 55 to 65% and occurred in the regions of current intensity 0.8 – 0.9 A (Fig. 1ab) H_2O_2 concentration of 0 – 600 mg L^{-1} (Fig. 1bc), and flow rate 0.6 – 0.8 L min^{-1} (Fig. 1ac). In order to minimize the formation of more selective and less oxidative radicals, such as hydroperoxyl ($HO_2^{\bullet}$) and ensure good efficiency of PEF process in hydroxyl radical production ($^{\bullet}OH$) and subsequent

of pollutants persistent in LL, the values of 300 mg H_2O_2 L^{-1}, current intensity of 0.9 A and flow rate of 0.6 L min^{-1} were adopted as optimum conditions of ROP.

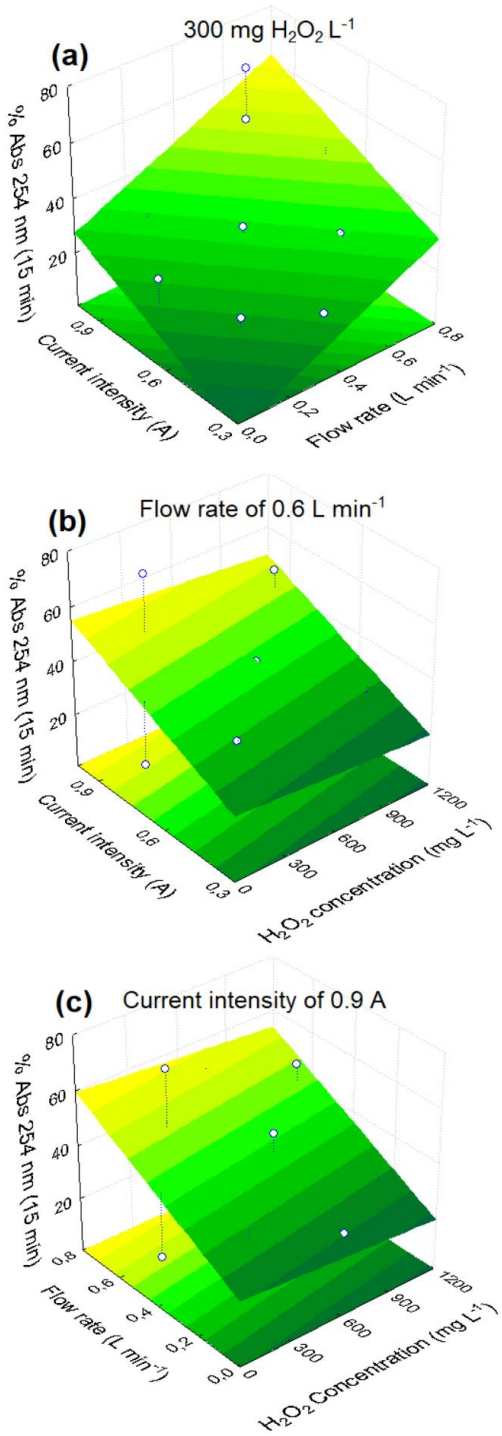

Figure 1. Response surface of the PEF process based on Abs 254 nm removal from LL.

3.3.4 Study of different anodes of the PEF process

3.3.4.1 Abs 254 nm, COD and TC removal kinetics

The removals of Abs 254 nm, COD and TC were assessed for BDD and soft iron anodes, applying the best experimental conditions of the PEF process, obtained from the RSM (Fig. 2).

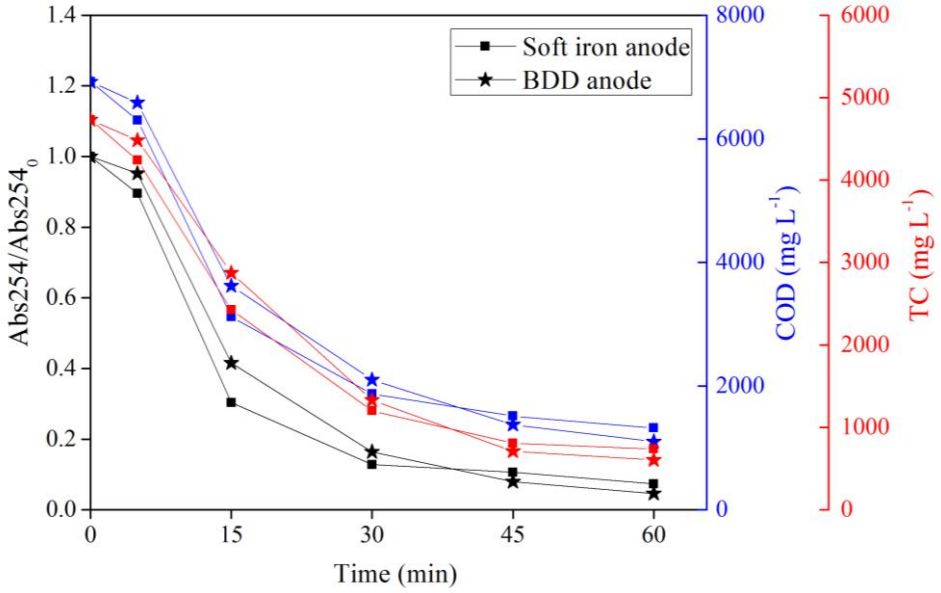

Figure 2. Abs 254 nm, COD and TC removal by the PEF under the operating conditions of pH 4-5, 300 mg H_2O_2 L^{-1}, Q = 0.6 L min^{-1} and I = 0.9 A.

As shown in Fig. 2, a significant reduction of Abs 254 nm was observed for both tested anodes, indicating a degradation of compounds with aromatic rings, especially humic acids (DIA et al., 2017). The reductions of COD and TC suggest a degradation and mineralization of the organic load present in LL. A higher removal rate of the studied parameters was observed in the first 30 min of PEF process. Similar behavior, of higher organic load abatement in the initial stages of the process was reported by other researchers and may be related to the higher availability of pollutants in solution at the beginning of the process (ATMACA, 2009; BORBA et al., 2019; DIA et al., 2017; LEI et al., 2007; SEIBERT et al., 2019b). Comparing the two types of anodes, it was verified that the soft iron anode presented a higher efficiency than the BDD anode in the removal Abs 254 nm, COD and TC up to 30 min of process. This may be related

to initial higher amounts of Fe^{2+} in solution due to dissolution of the anode material, contributing to the Fenton reaction kinetics (BRILLAS; SIRÉS; OTURAN, 2009; MOREIRA et al., 2017), or with the complexation and precipitation of organic compounds with iron ions (BAIJU et al., 2018; MOLLAH et al., 2001). After 30 min of process, the BDD anodes showed a higher efficiency in the removal of Abs 254 nm, COD and TC. This is suggested to be related to the great amounts of $^{\bullet}OH$ that this type of anode provides to the process (PANIZZA; CERISOLA, 2005). BDD electrodes are considered the most powerful non-active anodes known for electrochemical oxidation, producing $^{\bullet}OH$ radicals weakly physiosorbed on its surface, which remain available in high rates for the oxidation of organic compounds present in solution (ALFARO et al., 2006)

3.3.4.2 Genotoxicity assays

The genotoxic assays using the bioindicator *A. cepa* showed that the number of cells in division (MI) in 15 min PEF treatment using BDD anode is the closest of the values found in the distilled water control, with a T-value of 6.34272, indicating that this treatment condition presented the highest genotoxicity reduction (Table 2).

Table 2. Statistical comparison of number of cells in division observed in the control sample with the different samples of LL (3 counts of 1000 cells), applying T-test ($p < 0.05$).

Comparison	**T-value**	**p-value**
Control - Raw LL	14.89630	0.000118
Control - PEF 15 min (soft iron anode)	11.41589	0.000336
Control - PEF 30 min (soft iron anode)	15.29715	0.000107
Control - PEF 60 min (soft iron anode)	17.42883	0.000064
Control - PEF 15 min (BDD anode)	6.34272	0.003164
Control - PEF 30 min (BDD anode)	9.44730	0.000700
Control - PEF 60 min (BDD anode)	8.80051	0.000920

The other treatments presented higher levels of chromosomal damage and alterations in the stages of mitosis. Nevertheless, the *A. cepa* cells exposed to the LL treated using BDD anode for 15 min presented significant cell damage, such as

stickiness, c-mitosis, anaphasic bridge, micronuclei, necrosis and apoptosis, as showed in Fig. 3, suggesting that the sample still contains compounds that interact with the DNA and deregulate mitotic spindle fibers, leading to a low rate of cell division and numerous nuclear alterations (LEME; MARIN-MORALES, 2009).

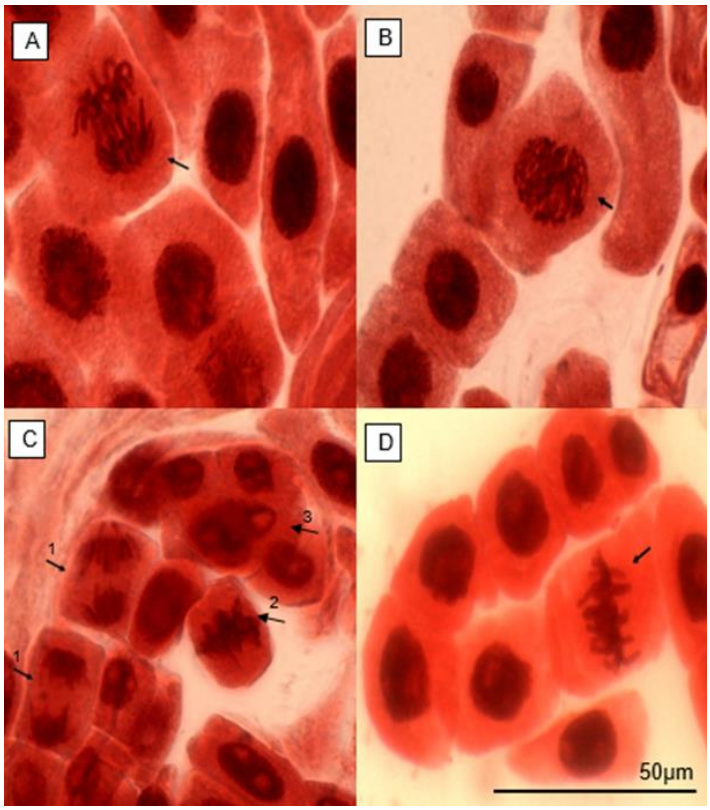

Figure 3. Different mitotic phases of *A. cepa* after its exposure to LL treated by PEF process: (**A**) irregular anaphase (anaphasic bridge), (**B**) abnormal prophase (chromosome folding), (**C**) [1] telophase isolated chromosome (micronuclei) [2] abnormal metaphase (stickiness) [3] apoptosis (**D**) abnormal metaphase (stickiness).

Table 3 presents the values of MI and abnormalities, evidencing that in all treatment times, with both iron and BDD anode, there was alteration in the cellular events of this eukaryotic organism, and that a reduction of the genotoxicity occurred in 15 min treatment with BDD anode, in comparison with the other treatment conditions.

Table 3. Mitotic index and percentage of abnormalities in the *A. cepa* genotoxicity assays.

Sample	Mitotic index (%)	Abnormalities (%)
Control	13.3	7.3
Raw LL	3.6	36.1
PEF 15 min (soft iron anode)	5.4	36.0
PEF 30 min (soft iron anode)	3.7	38.7
PEF 60 min (soft iron anode)	2.6	34.2
PEF 15 min (BDD anode)	9.3	48.4
PEF 30 min (BDD anode)	5.3	66.0
PEF 60 min (BDD anode)	6.0	70.7

The intermediate byproducts generated during the PEF process may be responsible for the cellular damage found in all treatment times, since many molecules present are potentially mutagenic as for example BPA and DBA, that are present even in the sample treated with BDD anode for 15 min (see Tables 2SM, 3SM and 4SM).

3.3.4.3 Phytotoxicity assays

Different dilutions of the untreated and PEF-treated LL were subjected to phytotoxicity tests with *L. sativa*. The results of GI, RGRI and HGRI are presented in Figure 4.

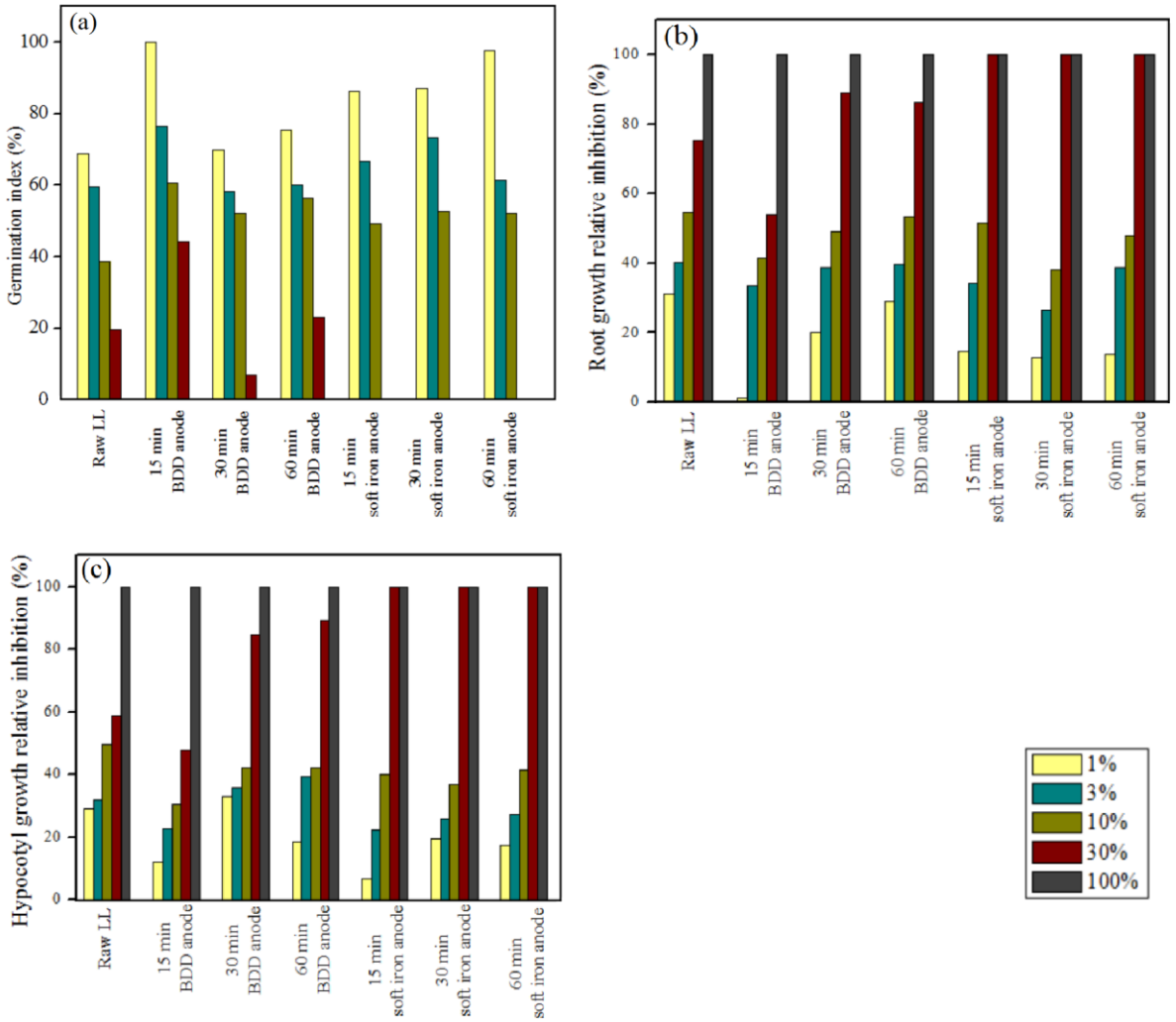

Figure 4. Phytotoxic effects of untreated and PEF-treated LL samples in germination and growth of *L. sativa*.

The raw LL caused high reduction in the germination index of *L. sativa* seeds, especially in the lower dilutions (Fig. 4a). These phytotoxic effects are also observed by the root and hypocotyl growth inhibitions, that increased for lower dilutions of raw LL (Fig. 4bc). This can be attributed to the toxic compounds identified in the LL (see Table 2SM). Additionally, the heavy metals and other elements present in the LL, which include S, Cl, K, Ca, Ti, V, Cr, Mn, Fe, Ni, Cu, Zn, Br, Sr and Pb (see Table 5SM), may cause phytotoxicity in *L. sativa*. Researches report that some heavy metals such as Mn, Fe, Cu, Zn, and Ni, are essential or beneficial for plants, however, at high concentrations, all heavy metals have toxic effects in living organisms (NEDELKOSKA; DORAN, 2000; WELCH; SHUMAN, 1995). The bioassays with treated samples

suggested that the highest reduction in the phytotoxicity occurred in 15 min of PEF treatment with BDD anode. This can be observed by an increase in the GI for the dilutions 1, 3, 10 and 30% (Fig. 4a), which could be related to the degradation of toxic compounds present in raw LL, such as 2-ethoxyethyl ether, linalyl oxide, DIOP, DEET, DBA and BPA (see Tables 2SM and 3SM). In addition, this treatment condition also caused lower inhibition in the growth of roots and hypocotyls, as shown in Fig. 4bc. Furthermore, higher treatment times by the PEF process with BDD anode caused a slight increase in the phytotoxicity, possibly due to formation of toxic byproducts of the oxidation processes and to the increase of iron species in solution, coming from the cathode material (ANGLADA et al., 2010).

The PEF process using soft iron anode promoted an increase in the phytotoxicity to *L. sativa*, which was clearly observed in the 30% dilution of the treated samples, decreasing the GI, and increasing RGRI and HGRI (Fig. 4). This increase in the toxicity could be related to an increase of iron in solution, coming from the dissolution of the electrodes' material. Excess of iron species in solution, as well as complexes formed by this metal, may cause toxic effects on living organisms development (WELCH; SHUMAN, 1995; ZHUANG et al., 2019). Another possible explanation for the increase in the phytotoxicity with higher times of PEF process is the formation of organochlorine compounds, that usually have high levels of toxicity (DE PAULI et al., 2017). Part of the chorine species present in the LL can be converted into hypochlorite (OCl^-) by electro-oxidation reactions, which can oxidize the organic matter, leading to the formation of organochlorine compounds (ANGLADA et al., 2010; BASHIR et al., 2013).

3.3.4.4 GC-MS analysis

The compounds detected by GC-MS after the treatments performed with different anodes, soft iron and BDD, are presented in the supplementary material (see Tables 2SM, 3SM and 4SM).

In both anodes' treatments the compound Tetracosane (RT 11.99 min) persisted during the whole process. Tetracosane is a component of volatile oils from plants and presents cytotoxicity toward colon, estrogen-dependent breast and gastric

cancer cells (UDDIN; GRICE; TIRALONGO, 2012), highlighting its recalcitrant characteristics. Employing BDD anode, the compound 3-Heptadecanol (RT 4.7 min) also persisted until the end of the process. Compounds of this class have been identified in avocado leaves and did not present significant toxicity (LEE et al., 2012).

Regarding the soft iron anodes some compounds were formed in 15 min of PEF process and were not removed along the whole process. These compounds are 1,4-diethylpiperazine (RT 4.64 min), 2-octadecoxyethanol (RT 5.84 min) and eicosane (RT 8.67 min). 1,4-diethylpiperazine has been characterized as corrosive and irritating to the skin or eyes of animals (ECHA, 2019). 2-octadecoxyethanol is an emulsifier used in cosmetic formulation (SAŁEK; EUSTON, 2019). Eicosane is classified by EPA (USEPA, 2012) as an EDC. This compound is an alkane, commonly detected in LL (KHALIL et al., 2018; KLAUCK et al., 2017; SEIBERT et al., 2019b), and it is mainly used in cosmetics and petrochemical industry (KANNO; FURUYAMA; HIRANO, 2008). In 30 minutes of electrolysis tetratriacontane (RT 6.87 min) was formed and persisted through the whole treatment. According to Ra et al. (2016), alkanes such as tetratriacontane, represent the second highest chemical group that contributes to toxicity of wastewaters. This compound was also detected in a LL by Hu et al., 2016, and persisted after an electro-oxidative process with BDD anode, as reported by Zhu et al. (2011). During the PEF process with soft iron anodes some byproducts were formed, especially in 30 minutes of electrolysis, where the highest number of compounds was identified (see Table 4SM) in parallel with a substantial reduction of the organic load. This may be related to the breakdown of aromatic rings, represented by the reduction of Abs 254 nm in the LL.

When BDD anodes were employed, heneicosane (RT 8.67 min) was formed in 15 min of process, and (1-Propylnonyl)cyclohexane (RT 9.78 min) in 30 min. Heneicosane is an EDC (USEPA, 2012) and was also detected in LL samples submitted to a photo-electro-oxidation process, being classified as a byproduct (KLAUCK et al., 2017). To the best of our knowledge, no information on the hazards and toxic effects of (1-Propylnonyl)cyclohexane has been reported in literature. The highest number of identified compounds in the treatment with BDD anode occurred in 60 min of process (see Table 3SM). This may be related to the breakdown and rearrangement of organic molecules, promoted by the PEF process, forming these

byproducts. It is noteworthy, that even though the soft iron anode was more efficient than BDD anode in 15 min of process (see Fig. 2), the genotoxicity and phytotoxicity tests indicated that the byproducts produced by the system with BDD anode were less toxic at this process time (see sections 3.3.4.2 and 3.3.4.3).

3.3.5 PEF process and biological oxidation (BO) integration

3.3.5.1 Microbial growth and TC and COD removals

Evaluations were performed by integrating PEF-BO and BO-PEF. When PEF pre-treated LL was applied to BO (PEF-BO integration), increases on optical density were observed, as well as oxygen consumption (Fig. 5a). This indicates microbial growth, which exhibited the typical growth phases in batch systems (MAUERHOFER et al., 2019). After a 6-h lag period, microbial growth (exponential phase) occurred until the stationary phase was reached (20 h), which proceeded until ~36 h of BO (Fig. 5a). Microbial growth was sustained by the consumption of provided substrates (PEF pre-treated LL), as indicated by decreases in TC and COD during BO (Fig. 5bc). TC and COD removals occurred mainly up to 40 h of BO, coinciding with a higher microbial biomass in the bioreactors (Fig. 5a). At this point, TC and COD presented reductions of 50% and 70% of the initial values, respectively. Applying longer BO (> 40 h), optical density and oxygen consumption decreased (Fig. 5a) and the concentrations of TC and COD in solution remained nearly constant up to 72 h, which may indicate the higher recalcitrance (or lower accessibility) of the remaining organic fraction to BO.

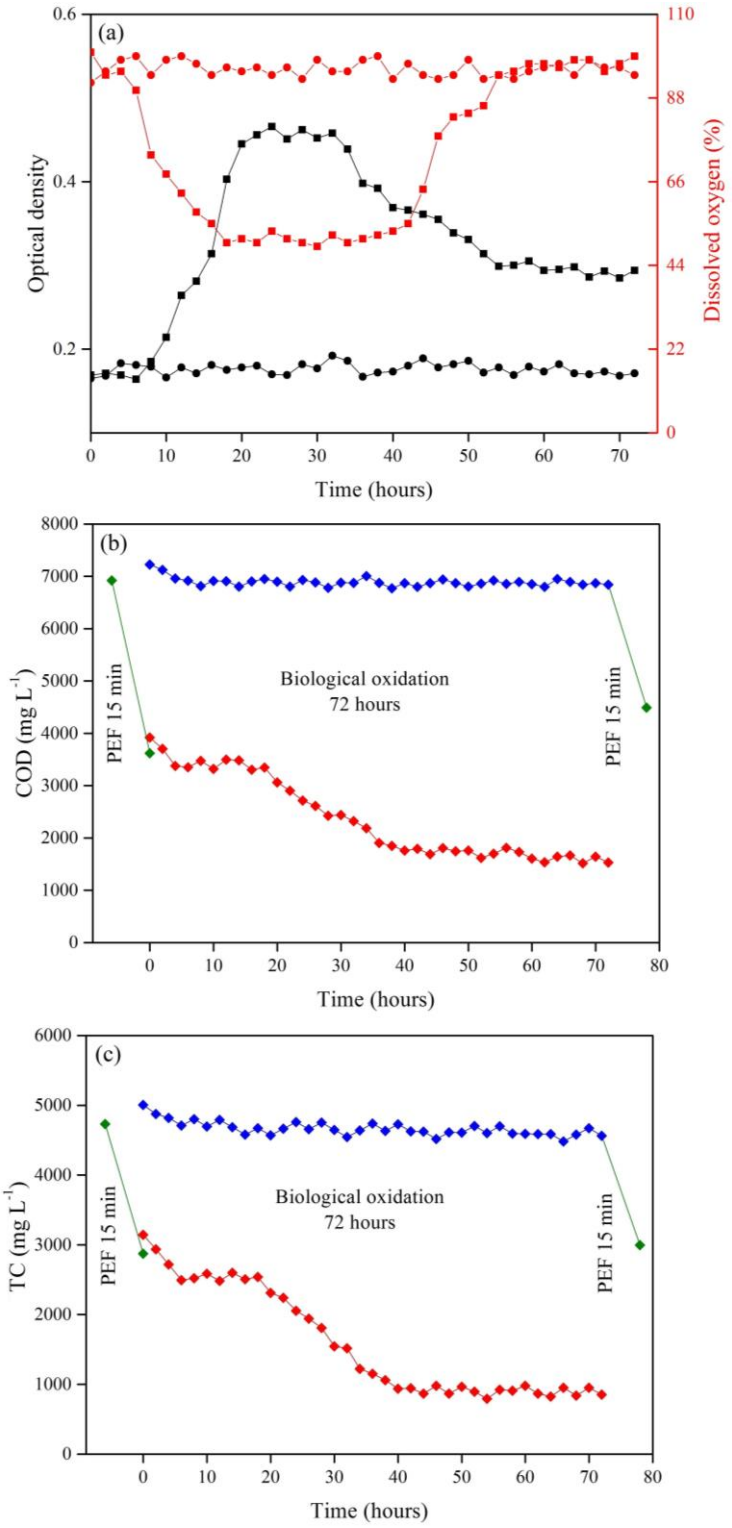

Figure 5. Optical density and dissolved oxygen in the biological oxidation processes applied to raw LL (●) and PEF pre-treated LL (■) (a); TC (b) and COD (c) removals by process integrations. PEF-BO integrations (red symbols) and BO-PEF integration (blue symbols).

On the other hand, when raw LL was submitted to BO (BO-PEF integration), no microbial growth was detected by optical density and dissolved oxygen was not consumed (Fig. 5a). Furthermore, TC and COD removals were negligible during BO in this integration strategy. This might have occurred due the toxicity of raw LL towards the BO inoculum, which is a complex microbial community composed by bacteria, fungi and protozoa (SEIBERT et al., 2019b), reinforcing the results obtained in toxicity tests (see Table 3 and Fig. 4.). The subsequent 15-min PEF treatment presented similar TC and COD values to those measured after PEF in the PEF-BO integration (Fig. 5bc). Thus, integration of the 15-min treatment by BDD-based PEF process, followed by BO (PEF-BO), was considered as the most suitable for LL treatment.

Furthermore, the relatively high TN levels (see Table 1) did not inhibit significantly the BO process, possibly due the conditions of the system: pH 7 and high organic load, which reduce the presence/formation of nitrogen forms that impair the microbial activity, such as ammonia, nitrate and nitrite (DEZZOTI; LIPPEL; BASSIN, 2018). Additionally, air stripping technique could be applied for the removal of nitrogen, aiming to improve the efficiency of BO, as reported by Inglezakis et al. (INGLEZAKIS et al., 2018).

3.3.5.2 Genotoxicity assays

A. cepa genotoxicity assays were also performed in the samples treated by the integration BO process (72 h) and PEF process (15 min) using BDD anode (Table 4).

Table 4. Mitotic index and abnormalities in cell division of *A. cepa* exposed to the samples treated by integrated processes.

Sample	Mitotic index (%)	Abnormalities (%)
Control	13.3	7.3
Raw LL	3.6	36.1
BO + PEF	4.8	36.5
PEF + BO	8.3	17.3

The integration strategy PEF-BO showed to be most efficient in the reduction of genotoxic effects of LL. This system increased the mitotic index o *A. cepa* root cells from 3.6 to 8.3%, reaching 62.8% of the mitotic index observed in the distilled water control solution. Additionally, the application of PEF-BO promoted a reduction in 47.8%

in the abnormalities observed in cell division (Table 4). Furthermore, the use of BO-PEF process showed to be less efficient in the degradation of genotoxic compounds presented in LL, presenting no substantial alteration in the mitotic index and abnormalities, in comparison with raw LL.

3.3.5.3 Phytotoxicity assays

The reduction in phytotoxicity of LL by the integration of 72 h BO with 15 min PEF process under the best operation condition, with BDD anode, was assessed and presented in Figure 6.

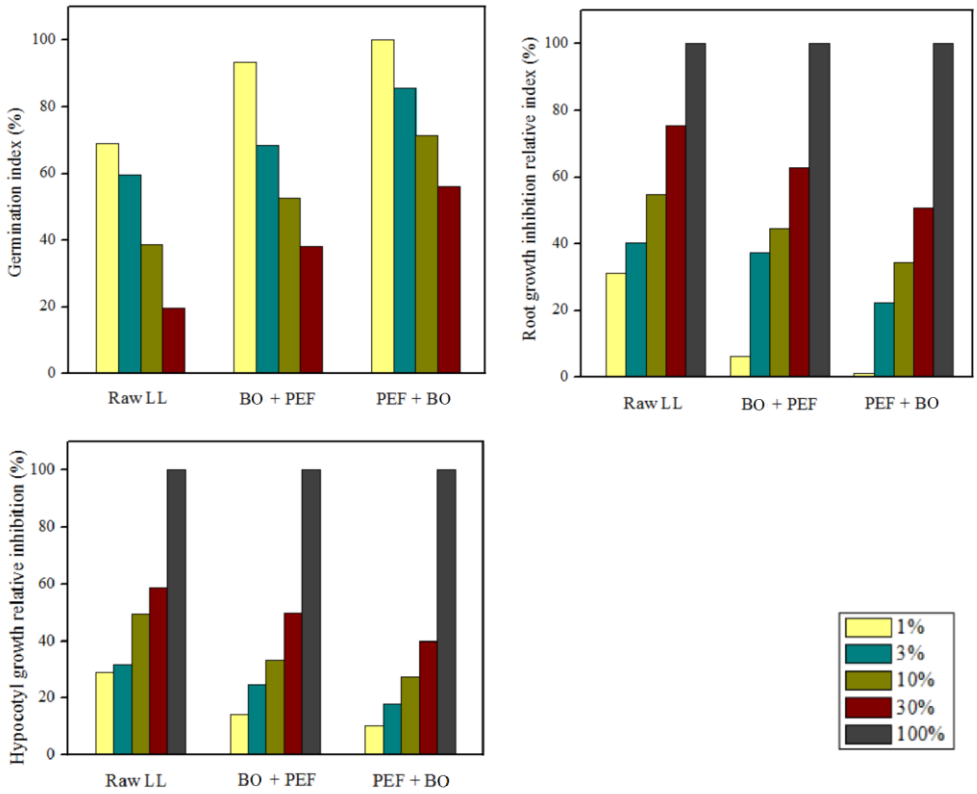

Figure 6. Phytotoxicity bioassays on the integrated treatment process.

The phytotoxicity results indicated the same trend as the COD and TC removal (see Fig. 5bc), showing a higher efficiency in the reduction of toxic effects by the application of PEF-BO in comparison with the system using the inverse order of processes (BO-PEF). It can be suggested that this is related to the higher degradation of the organic load of LL that this configuration has promoted, which include the degradation and mineralization of toxic compounds. Similar behavior of toxicity

reduction comparing different configurations PEF process integrated with BO were observed by (SEIBERT et al., 2019b). The remaining phytotoxicity may be related to metals that were not removed by the processes, such as Fe (see Table 5SM), as well as to byproducts of the processes, that even in low concentrations, may cause toxic effects to living organisms.

3.3.5.4 GC-MS analysis

An investigation of the byproducts formed in the PEF and BO combined treatment strategies was also carried out, and presented in Table 6SM.

Advanced oxidation processes are known to be able to transform recalcitrant compounds into low-molecular organic compounds which may have their biodegradability index increased (MANDAL; DUBEY; GUPTA, 2017). For this reason, a pre-treatment with PEF increased the biodegradability and reduced the toxicity of the LL, making it more suitable for BO. In the integrated system PEF-BO, the following compounds were detected: Isoamyl acetate (RT: 4.17 min), 2,4-Di-tert-butylphenol (RT: 5.89 min), Eicosane (RT: 11.71 min), Tetracosane (RT: 11.97), 2-Methylnonane (RT: 17.13 min) and Tetratetracontane (RT: 21.77 min). Isoamyl acetate is a metabolite of microorganisms (CHEBI, 2019), also used as a flavor food addictive (EU, 2012). 2,4-Di-tert-butylphenol is a byproduct from the degradation of phosphonite-based antioxidants, also reported as an estrogenic compound (LIU; YIN; DANG, 2017; LÖSCHNER et al., 2011). Eicosane is considered an EDC, as previously described (USEPA, 2012). Tetracosane persisted from the raw LL in all the experimental conditions. There is still a lack of information about the safety and hazards of 2-Methylnonane in the literature, however is classified as aspiration hazardous (ECHA, 2019). Regarding to Tetratetracontane, which is a long chain alkane, to the best of our knowledge, there is no information about its possible toxic effects in literature.

On the other hand, the integration strategy BO-PEF was less efficient in the removal of organic compounds and toxicity. In this integration strategy microbial cultures possibly acted as $^{\bullet}OH$ scavenger, decreasing oxidative potential of PEF process (SEIBERT et al., 2019b). Additionally, the biological degradation of the organic compounds may have been inhibited by the toxic and recalcitrant characteristics of the

raw LL. Thus, the GC-MS analysis identified the following byproducts of this treatment system: 1-[methoxy]-2-heptadecanone (RT: 4.62 min), 1-Pentadecanesulfonic acid (RT: 4.93 min), 2(3H)-Furanone, dihydro-5,5-dimethyl-4-(3-oxobutyl) (RT: 5.60 min), DBA (RT: 5.95 min), Octadecane (RT: 6.83 min), Tetratriacontane (RT: 7.60 min), Tricosylradical (RT: 8.43 min), 2-Hydroxytricosanoic acid (RT: 9.67 min), BPA (RT: 11.46 min) and Tetracosane (RT: 11.97 min). Several of these compounds were also identified via GC-MS analysis in the 15 min BDD anode-treated LL and some of them were detected also in the raw LL, such as DBA and BPA. Based on this information it can be suggested that in this treatment strategy, the BO process had little influence in the removal of pollutants from LL.

3.4. CONCLUSIONS

LL is a wastewater with high pollution potential, toxicity and recalcitrant characteristics, making its treatment a challenge for managers. Therefore, a BDD-based PEF system integrated to an aerobic BO process was proposed and investigated. The best integration system was achieved with a 15-min PEF pre-treatment using 300 mg H_2O_2 L^{-1}, 0.9 A current intensity and system flow rate of 0.6 L min^{-1}, followed by a 72-hours activated sludge BO process. This treatment strategy promoted reductions of 77.9%, 71.5%, and 76.3% of COD, TC and Abs 254 nm, respectively, as well as reductions in genotoxicity, verified by an increase of 131.5% in the MI and a decrease of 47.8% in the abnormalities. GC-MS analysis indicated the degradation of several potentially hazardous compounds present in the raw LL by the PEF-BO treatment strategy, highlighting the emerging contaminant BPA. Thus, the integration of BDD-based PEF process with BO is presented as a relevant alternative, providing efficiency and low cost to LL treatment, aiming to minimize the toxic effects of this effluent on the environment.

ACKNOWLEDGMENTS

The authors wish to thank CNPq Universal (429116/2016-0), FAPERGS/CAPES (05/2017), FAPERGS/CAPES (03/2018) and FAPERGS (05/2019) for the financial support of this study.

SUPPLEMENTARY MATERIAL

LIST OF SUPPLEMENTARY FIGURES

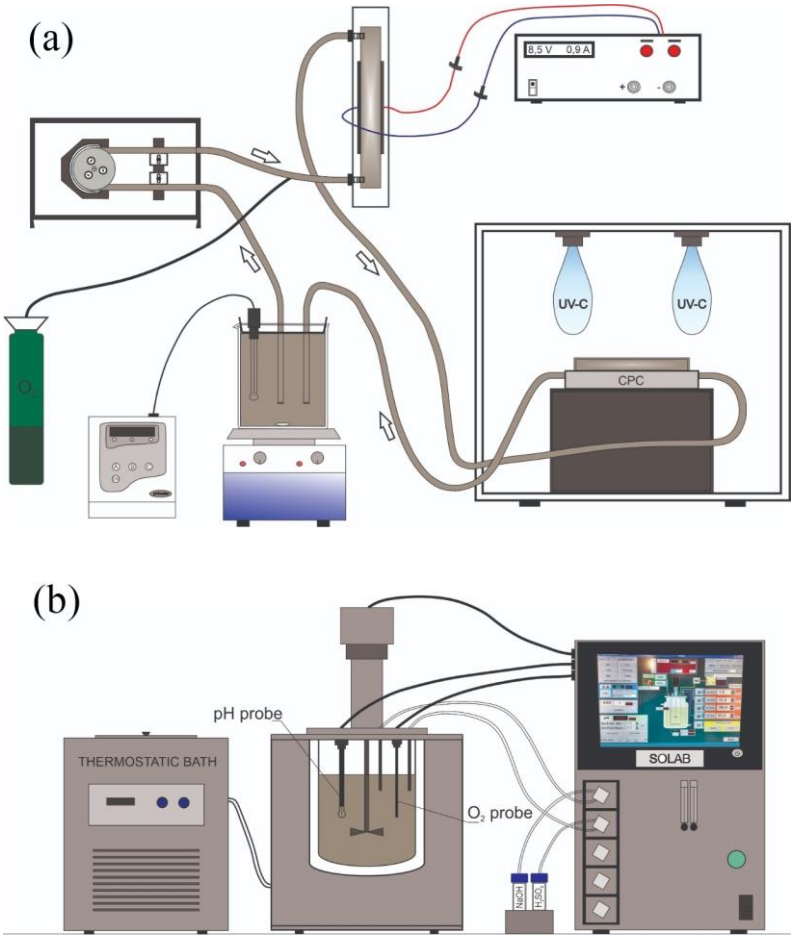

Figure 1SM. PEF reactor (a) and BO reactor (b).

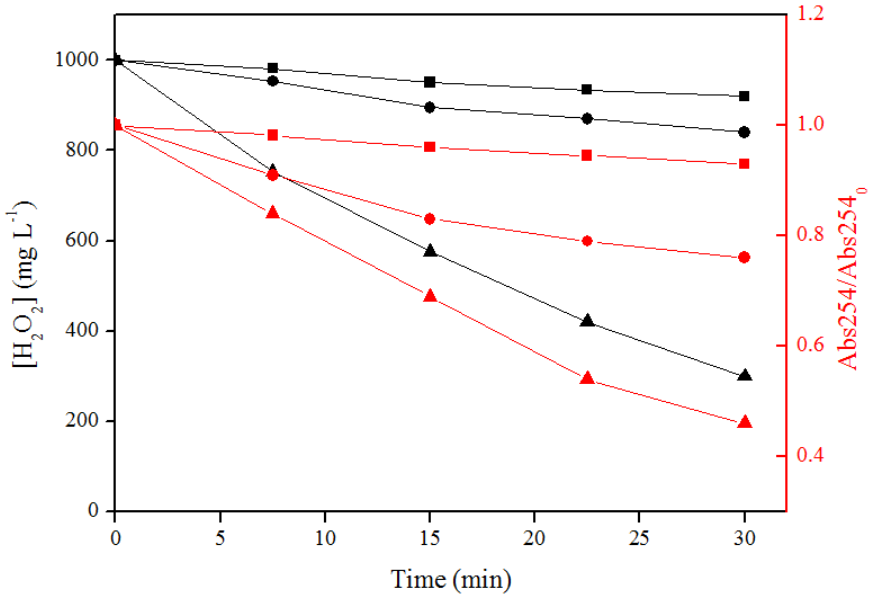

Figure 2SM: Analysis of H_2O_2 consumption (no reposition) and Abs 254 nm removal under the following conditions: absence of UVC radiation and current intensity (■), presence of UVC radiation and absence of current intensity (●), presence of UVC radiation and 0.5-A current intensity (▲).

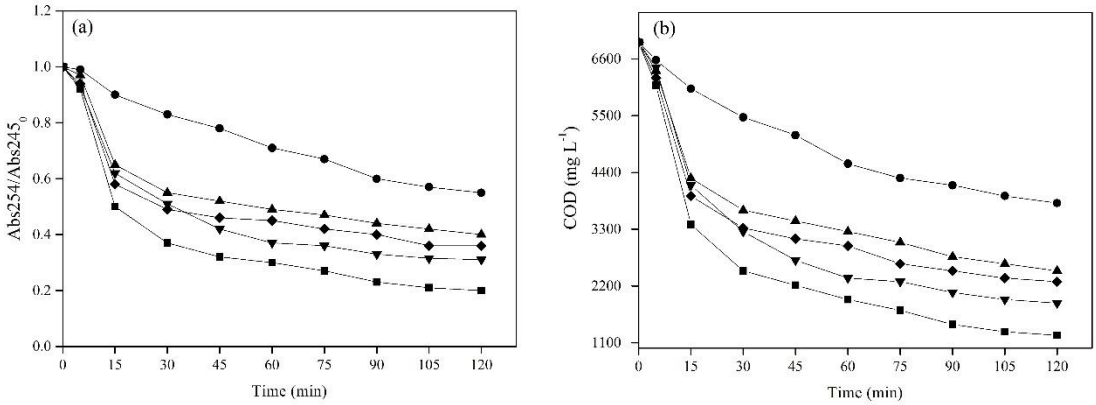

Figure 3SM. Preliminary tests of the PEF system using pH 4 – 5, and varying the following operational conditions: O_2 rate = 0.2 L min^{-1}, UVC radiation, $[H_2O_2]$ = 1000 mg L^{-1}, I = 0.5 A (■); O_2 rate = 0.2 L min^{-1}, UVC radiation, I = 0.5 A (♦); O_2 rate = 0.2 L min^{-1}, $[H_2O_2]$ = 1000 mg L^{-1}, I: 0.5 A (▲); O_2 rate = 0.2 L min^{-1}, UVC radiation, $[H_2O_2]$ = 1000 mg L^{-1} (●); UVC radiation, $[H_2O_2]$ = 1000 mg L^{-1}, I = 0.5 A (▼).

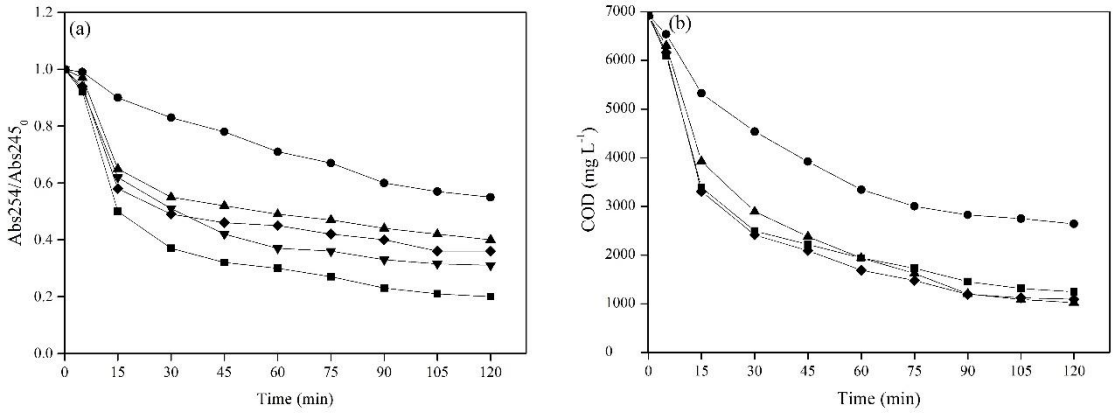

Figure 4SM. Preliminary tests using pH 4 – 5, 0.2 L O_2 min^{-1}, UVC radiation, and varying the ROP to be investigated by the RSM: [H_2O_2] = 1000 mg L^{-1}, I = 0.5 A, Q = 0.2 L min^{-1} (■); [H_2O_2] = 500 mg L^{-1}, I = 0.5 A, Q = 0.2 L min^{-1} (♦); [H_2O_2] = 500 mg L^{-1}, I = 0.5 A, Q = 0.8 L min^{-1} (▲); [H_2O_2] = 1000 mg L^{-1}, I = 0.2 A, Q = 0.2 L min^{-1} (●).

LIST OF SUPPLEMENTARY TABLES

Table 1SM. Performance of the CCRD in the removal of Abs 254 nm by PEF process.

				Abs 254 nm removal (%)			
Run	H_2O_2 concentration (mg L^{-1}) (q_1)	Current intensity (A) (q_2)	Flow rate (L min^{-1}) (q_3)	PEF 15 min	PEF 30 min	PEF 45 min	PEF 60 min
1	300	0.9	0.2	25.0	48.0	57.0	65.0
2	1372.7	0.7	0.4	21.0	32.0	39.3	46.7
3	700	0.7	0.06	25.0	41.5	52.1	59.3
4	300	0.5	0.6	30.8	41.0	49.0	53.0
5	700	0.36	0.4	18.2	26.9	39.7	44.6
6	1100	0.5	0.2	17.0	30.0	38.4	49.3
7	27.3	0.7	0.4	18.0	38.9	47.9	53.8
8	700	0.7	0.4	30.0	51.0	61.0	67.0
9	300	0.9	0.6	65.5	77.0	82.3	85.0
10	700	0.7	0.74	38.0	57.0	65.0	69.3
11	700	0.7	0.4	28.3	48.7	62.3	68.1
12	700	1.04	0.4	45.0	59.3	67.2	73.4
13	300	0.5	0.2	17.0	29.0	38.0	43.0
14	1100	0.9	0.2	19.0	45.0	52.0	61.0
15	1100	0.9	0.6	47.0	67.0	74.0	81.0
16	1100	0.5	0.6	25.0	41.0	52.0	58.0
17	700	0.7	0.4	29.1	47.5	62.1	67.9

Table 2SM: Raw LL GC-MS analysis.

RT (min)	Molecular formula	Molecular structure	CAS number
4.19	$C_8H_{18}O_3$	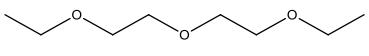	112-36-7
4.27	$C_6H_{12}O_3$	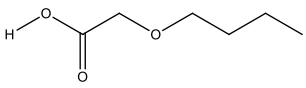	2516-93-0
4.43	$C_9H_{18}O_2$	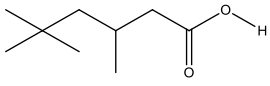	3302-10-1

RT (min)	Molecular formula	Molecular structure	CAS number
4.70	$C_{10}H_{18}O_2$	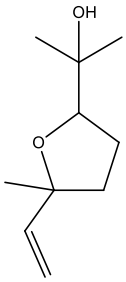	5989-33-3
4.86	$C_{10}H_{18}O$	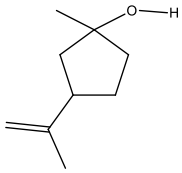	4028-60-8
4.91	$C_{10}H_{16}O_3$	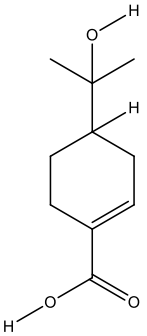	5027-76-9
5.29	$C_{24}H_{38}O_4$	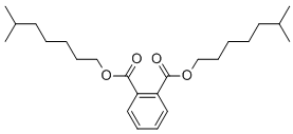	27554-26-3
5.88	$C_{12}H_{17}NO$	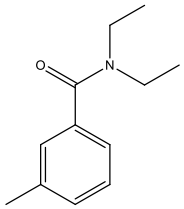	134-62-3
6.00	$C_9H_{10}O_4$	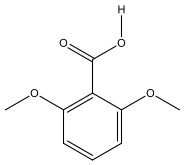	1466-76-8
6.25	$C_{17}H_{26}O_2$	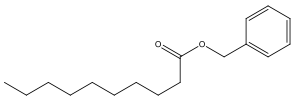	42175-41-7
9.81	$C_{26}H_{52}$		18835-33-1
10.09	$C_{20}H_{42}$	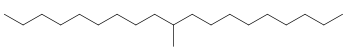	56862-62-5

RT (min)	Molecular formula	Molecular structure	CAS number
11.53	$C_{15}H_{16}O_2$	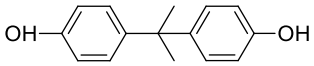	80-05-7
11.99	$C_{24}H_{50}$		646-31-1

Table 3SM: GC-MS analysis of LL treated by PEF process using BBD anode.

RT (min)	Molecular formula	Molecular structure	CAS number
		15 min treatment	
4.63	$C_{23}H_{44}O_4$	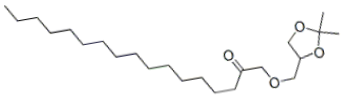	39033-40-4
4.7	$C_{17}H_{36}O$	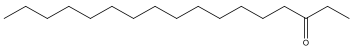	84534-30-5
4.98	$C_{15}H_{32}O_3S$	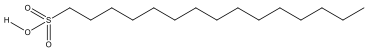	31169-63-8
5.18	$C_{18}H_{36}O$	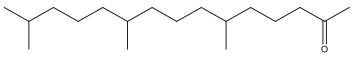	502-69-2
5.73	$C_{10}H_{16}O_3$	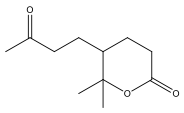	4436-81-1
6.00	$C_9H_{10}O_4$	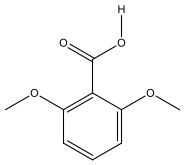	1466-76-8
6.29	$C_{20}H_{42}$	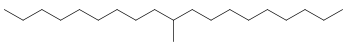	56862-62-5
6.86	$C_{18}H_{38}$		593-45-3
7.63	$C_{34}H_{70}$		14167-59-0
8.67	$C_{21}H_{44}$		629-94-7
9.70	$C_{23}H_{46}O_3$	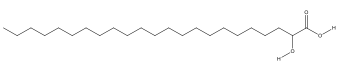	-
10.09	$C_{19}H_{40}$	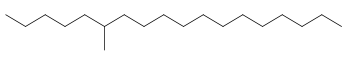	10544-96-4
11.45	$C_{15}H_{16}O_2$	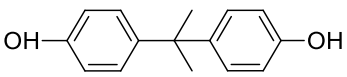	80-05-7

RT (min)	Molecular formula	Molecular structure	CAS number
11.99	$C_{24}H_{50}$		646-31-1
		30 min treatment	
4.10	$C_5H_8O_3$	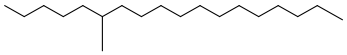	123-76-2
4.35	$C_4H_5NO_2$	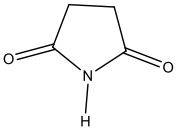	123-56-8
4.63	$C_6H_{10}N_2O_2$	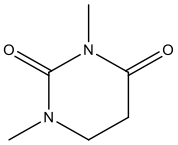	4874-13-9
4.7	$C_{10}H_{18}O_3$	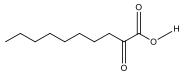	-
5.99	$C_9H_{10}O_4$	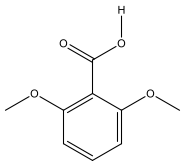	1466-76-8
6.29	$C_{20}H_{42}$	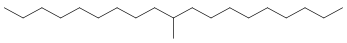	56862-62-5
6.87	$C_{34}H_{70}$		14167-59-0
7.62	$C_{27}H_{56}$		593-49-7
8.67	$C_{21}H_{44}$		629-94-7
9.78	$C_{18}H_{36}$	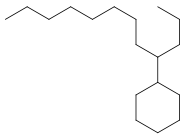	13151-84-3
10.09	$C_{44}H_{90}$		7098-22-8
11.99	$C_{24}H_{50}$		646-31-1
		60 min treatment	
4.33	$C_{20}H_{42}$	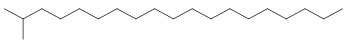	1560-86-7
4.64	$C_6H_{10}N_2O_2$	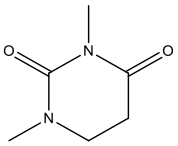	4874-13-9

RT (min)	Molecular formula	Molecular structure	CAS number
4.7	$C_{10}H_{18}O_3$	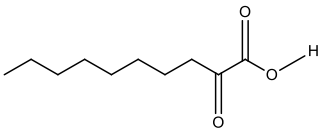	-
4.98	$C_{21}H_{40}O_4$	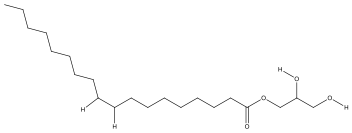	-
5.09	$C_{19}H_{40}$	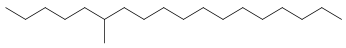	10544-96-4
5.37	$C_{27}H_{56}O$		2004-39-9
5.84	$C_{16}H_{34}$		544-76-3
6.28	$C_{34}H_{70}$		14167-59-0
6.86	$C_{20}H_{42}$		112-95-8
6.95	$C_{69}H_{138}O_2$	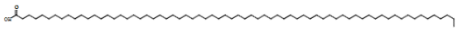	40710-32-5
7.63	$C_{20}H_{42}$	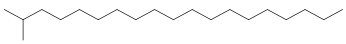	1560-86-7
8.17	$C_{16}H_{32}O_2$	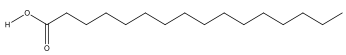	57-10-3
8.46	$C_7H_5NS_2$	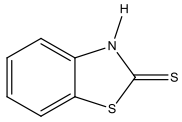	149-30-4
8.67	$C_{21}H_{44}$		629-94-7
9.67	$C_{48}H_{99}BO_3$	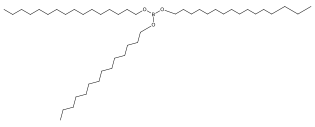	2665-11-4
9.78	$C_{18}H_{36}$	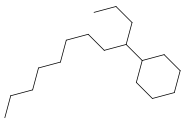	13151-84-3
9.99	$C_{12}H_{22}O$	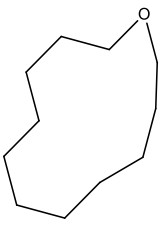	286-99-7

RT (min)	Molecular formula	Molecular structure	CAS number
11.62	$C_{19}H_{38}$	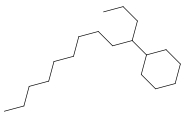	13151-89-8
11.99	$C_{24}H_{50}$		646-31-1

Table 4SM: GC-MS analysis of LL treated by PEF process using soft iron anode.

RT (min)	Molecular formula	Molecular structure	CAS number
		15 min treatment	
4.64	$C_8H_{18}N_2$	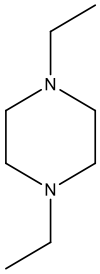	6483-50-7
4.70	$C_{10}H_{22}O_2$	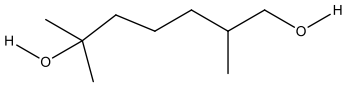	107-74-4
5.84	$C_{20}H_{42}O_2$		2136-72-3
6.28	$C_{69}H_{138}O_2$	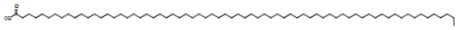	40710-32-5
6.86	$C_{20}H_{42}$	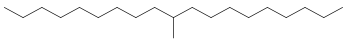	56862-62-5
7.63	$C_{34}H_{70}$		14167-59-0
8.67	$C_{20}H_{42}$		112-95-8
9.78	$C_{35}H_{70}$	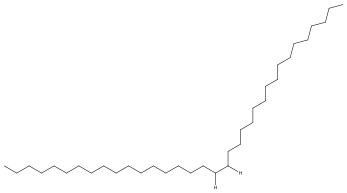	6971-40-0
11.99	$C_{24}H_{50}$		646-31-1
		30 min treatment	

RT (min)	Molecular formula	Molecular structure	CAS number
4.51	$C_8H_{10}O_2$	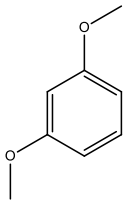	151-10-0
4.64	$C_6H_{10}N_2O_2$	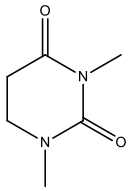	4874-13-9
4.69	$C_7H_8O_2$	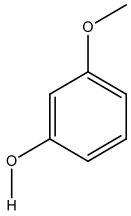	150-19-6
5.29	$C_{24}H_{38}O_4$	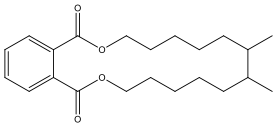	27554-26-3
5.84	$C_{16}H_{34}$		544-76-3
6.00	$C_9H_{10}O_4$	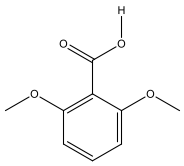	1466-76-8
6.08	$C_8H_7NS_2$	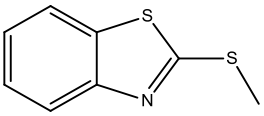	615-22-5
6.28	$C_{20}H_{42}$	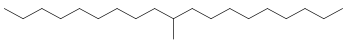	56862-62-5
6.87	$C_{34}H_{70}$		14167-59-0
7.63	$C_{27}H_{56}$		593-49-7
8.44	$C_7H_5NS_2$	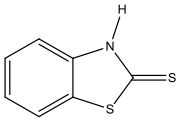	149-30-4
8.67	$C_{20}H_{42}$		112-95-8

RT (min)	Molecular formula	Molecular structure	CAS number
9.79	$C_{19}H_{38}$	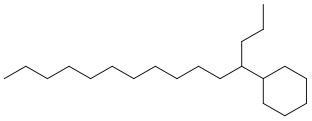	13151-89-8
10.09	$C_{35}H_{72}$		630-07-9
11.99	$C_{24}H_{50}$		646-31-1
		60 min treatment	
4.64	$C_8H_{18}N_2$	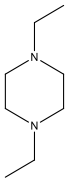	6483-50-7
5.84	$C_{69}H_{138}O_2$	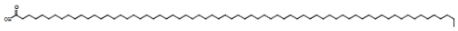	40710-32-5
6.29	$C_{34}H_{70}$		14167-59-0
6.87	$C_{18}H_{38}$		593-45-3
7.64	$C_{21}H_{44}$		629-94-7
8.67	$C_{41}H_{84}O$	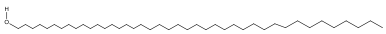	40710-42-7
9.80	$C_{19}H_{40}O$	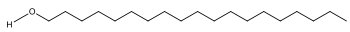	1454-84-8
10.08	$C_{20}H_{42}$		112-95-8
11.99	$C_{24}H_{50}$		646-31-1

Table 5SM. TXRF analysis of elements concentrations in the LL samples.

Element	Metallic elements in LL samples (mg L^{-1})					Limit of detection (mg L^{-1})
	Raw leachate	PEF 15min	PEF 15min + BO 72h	BO 72h	BO 72h + PEF 15min	
S	1642.553 ±2.481	2227.780 ±2.732	2176.773 ±2.314	1662.576 ±2.477	2347.176 ±3.120	1.436

Element	Metallic elements in LL samples (mg L^{-1})					Limit of detection (mg L^{-1})
	Raw leachate	PEF 15min	PEF 15min + BO 72h	BO 72h	BO 72h + PEF 15min	
Cl	1582.772 ±2.037	1731.514 ±1.840	1627.952 ±1.688	1594.106 ±1.800	1781.155 ±2,080	1.159
K	968.208 ±0.972	1092.882 ±0.984	1103.290 ±0.844	965.694 ±0.931	1087.771 ±1.145	0.448
Ca	95.602 ±0.229	97.478 ±0.219	104.543 ±0.196	94.439 ±0.225	95.784 ±0,264	0.105
Ti	0.528 ±0.020	0.593 ±0.022	0.263 ±0.015	0.464 ±0.018	0.245 ±0.020	0.036
V	0.262 ±0.014	0.228 ±0.015	0.221 ±0.013	0.267 ±0.014	0.224 ±0.015	0.028
Cr	0.500 ±0.014	0.446 ±0.015	0.294 ±0.012	0.512 ±0.014	0.315 ±0.014	0.023
Mn	1.182 ±0.017	1.170 ±0.020	1.162 ±0.015	1.143 ±0.015	0.158 ±0.019	0.025
Fe	11.032 ±0.040	80.600 ±0.101	49.515 ±0.072	9.564 ±0.033	78.994 ±0.088	0.025
Ni	0.236 ±0.006	0.250 ±0.006	0.189 ±0.005	0.204 ±0.005	0.198 ±0.006	0.009
Cu	0.085 ±0.005	0.310 ±0.006	0.228 ±0.005	0.078 ±0.004	0.302 ±0.006	0.009
Zn	0.762 ±0.008	0.788 ±0.009	0.324 ±0.005	0.714 ±0.007	0.732 ±0.007	0.012
Br	4.568 ±0.015	5.208 ±0.014	5.662 ±0.013	4.474 ±0.014	5.384 ±0.018	0.005
Sr	0.382 ±0.006	0.463 ±0.006	0.457 ±0.005	0.401 ±0.005	0.469 ±0.007	0.008
Pb	0.334 ±0.006	0.325 ±0.006	0.364 ±0.006	0.380 ±0.006	0.343 ±0.006	0.005

Table 6SM: GC-MS analysis of LL treated by the integration of PEF using BDD anode process with BO.

RT (min)	Molecular formula	Molecular structure	CAS number
		BO 72h + PEF 15 min	
4.62	$C_{23}H_{44}O_4$	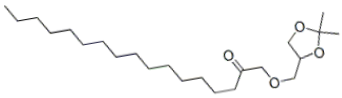	39033-40-4
4.93	$C_{15}H_{32}O_3S$	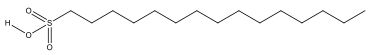	31169-63-8
5.60	$C_{10}H_{16}O_3$	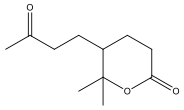	4436-81-1
5.95	$C_9H_{10}O_4$	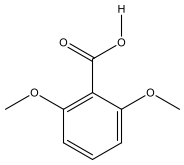	1466-76-8
6.83	$C_{18}H_{38}$		593-45-3
7.60	$C_{34}H_{70}$		14167-59-0
8.43	$C_{23}H_{47}$		-
9.67	$C_{23}H_{46}O_3$	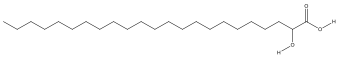	-
11.46	$C_{15}H_{16}O_2$	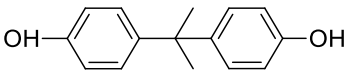	80-05-7
11.97	$C_{24}H_{50}$		646-31-1
		PEF 15 min + BO 72 h	
4.17	$C_7H_{14}O_2$	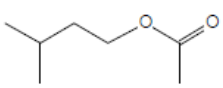	123-92-2

RT (min)	Molecular formula	Molecular structure	CAS number
5.89	$C_{14}H_{22}O$	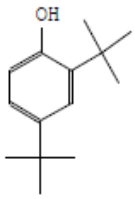	96-76-4
11.71	$C_{20}H_{42}$		112-95-8
11.97	$C_{24}H_{50}$		646-31-1
17.13	$C_{10}H_{22}$	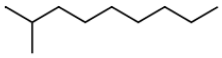	871-83-0
21.77	$C_{44}H_{90}$		7098-22-8

SUPPLEMENTARY METHODOLOGIES

Allium cepa genotoxicity assays

The *A. cepa* genotoxicity assays consisted in the exposure, in analytical triplicate, of bulbs to samples of the LL, in order to assess the adverse effects during cell mitosis. Bulbs with a diameter between 4 and 8 cm were placed in distilled water for 72 hours for rooting, and then, with meristem of approximately 3 cm, exposed to the samples and to the negative control (distilled water) for 72 hours in 50-ml glass vessels. After the exposure, the roots were removed from the bulbs and submerged in Carnoy's solution (75% ethanol and 25% acetic acid) for 24 hours, and then, stored in isopropyl alcohol (70%) under refrigeration. The preparation of the mitotic division analysis was carried out according to the Feulgen protocol, as described by Fiskesjö (FISKESJÖ, 1993). 3000 cells per sample were counted in an optical microscope (Optical Microscope Olympus® CX31) for mitosis and abnormalities evaluation. The

mitotic index (***MI***) was calculated by Equation 1, where NC_{div} is the number of cells in mitotic division and ***TNC*** is the total number of counted cells.

$$\mathrm{MI} = \left(\frac{\mathrm{NCdiv}}{\mathrm{TNC}}\right) \mathrm{x}\ 100 \quad (1)$$

Furthermore, the abnormality index was calculated by the percentage of divisions that presented anomalies.

Lactuca sativa phytotoxicity assays

L. sativa seeds-based phytotoxicity bioassays were performed following the methodology described by Sobrero and Ronco (SOBRERO; RONCO, 2004). Initially, dilutions of 0 (negative control), 1, 3, 10, 30, and 100%, of the treated and untreated LL samples were prepared in hard water stock solutions. 20 *L. sativa* seeds were exposed to 4 mL of each diluted sample, in analytical triplicate, in Petri dishes with filter paper on the bottom. After 120 h of incubation, at temperature of 22 ± 2 °C and absence of light, the number of germinated seeds was counted.

The germination index (***GI***), root growth relative inhibition (***RGRI***) and hypocotyl growth relative inhibition (***HGRI***) were calculated by Equations 2, 3 and 4, respectively.

$$\mathrm{GI} = \frac{\mathrm{NGS}}{\mathrm{NS}} \times \frac{\mathrm{RLA}}{\mathrm{RLAc}} \times 100 \quad (2)$$

$$\mathrm{RGRI} = \frac{\mathrm{RLAc} - \mathrm{RLA}}{\mathrm{RLAc}} \times 100 \quad (3)$$

$$\mathrm{HGRI} = \frac{\mathrm{HLAc} - \mathrm{HLA}}{\mathrm{HLAc}} \times 100 \quad (4)$$

Where ***NGS*** is the average number of germinated seeds in the diluted LL solution, NS is the total number of seeds, ***RLA*** is the root length average of the

samples, ***RLAc*** is the root length average of the negative control, ***HLA*** is the hypocotyl length average of the samples and ***HLAc*** is the hypocotyl length average of the negative control.

GC-MS analysis

Organic compounds present in the treated and untreated LL samples were identified through and analysis based in gas chromatography coupled to mass spectrometry. An extraction procedure was carried out using 3 x 20 mL CH_2Cl_2 in 40 mL of the samples. The extracted organic material was dried with anhydrous $MgSO_4$ and concentrated to 5 ml by rotary evaporation (Hei-VAP Precision, HEIDOLPH) with a temperature of 40 °C. Distilled water was subjected to the same procedure and used as blank solution.

The GC-MS analyses were carried out in an equipment (GCMS-QP2010, Shimadzu) equipped with a DB-5 MS column (30 m, 0.25 mm, 0.25 µm coating thickness), composed of dimethyl polysiloxene (95%) and diphenyl (5%). The injector and detector temperature was 280 °C, with interface temperature of 200°C. 1-µL samples were injected with a split ratio of 1:10 He gas at a flow rate of 1.65 mL min^{-1}. The temperature of the chromatograph was initially set to 50 °C, held constant for 7 min, then increased at a rate of 25 °C min^{-1} up to 280 °C and held for 20 min. The mass spectrometry was detected at a voltage of 0.97 kW, generating an electron impact ionization of 70 eV, which provided molecular fragmentation and ion production in a mass/electric charge (m/z) field of 25 – 500. The ion source temperature was set to 250 °C. Organic compounds present in the samples were identified based on their GC–MS patterns provided by the NIST 08 library available in GCMS-QP2010. Compounds with similarity percentage higher than 80% were reported as identified.

REFERÊNCIAS

ABNT. NBR 8419, Associação Brasileira de Normas Técnicas. . 1992.

ABRELPE. **Panorama dos resíduos sólidos no Brasil 2017**. [s.l: s.n.].

ALFARO, Marco Antonio Quiroz et al. Boron doped diamond electrode for the wastewater treatment. **Journal of the Brazilian Chemical Society**, [s. l.], v. 17, n. 2, p. 227–236, 2006.

ALLEN J. BARD, ROGER PARSONS, Joseph Jordan. **Standard Potentials in Aqueous Solution**. 1. ed. [s.l: s.n.].

ALVES, Suellen A. et al. Electrochemical degradation of the insecticide methyl parathion using a boron-doped diamond film anode. **Journal of Electroanalytical Chemistry**, [s. l.], v. 702, p. 1–7, 2013.

ANFRUNS, A. et al. Coupling anammox and advanced oxidation-based technologies for mature landfill leachate treatment. **Journal of Hazardous Materials**, [s. l.], v. 258–259, p. 27–34, 2013.

ANGLADA, Ángela et al. Boron-doped diamond anodic treatment of landfill leachate : Evaluation of operating variables and formation of oxidation. [s. l.], v. 5, 2010.

ANTONIN, Vanessa S. et al. Degradation of Evans Blue diazo dye by electrochemical processes based on Fenton's reaction chemistry. **Journal of Electroanalytical Chemistry**, [s. l.], v. 747, p. 1–11, 2015.

ASGHAR, Anam; ABDUL RAMAN, Abdul Aziz; WAN DAUD, Wan Mohd Ashri. Advanced oxidation processes for in-situ production of hydrogen peroxide/hydroxyl radical for textile wastewater treatment: a review. **Journal of Cleaner Production**, [s. l.], v. 87, p. 826–838, 2015.

ATMACA, Eyüp. Treatment of landfill leachate by using electro-Fenton method. **Journal of Hazardous Materials**, [s. l.], v. 163, n. 1, p. 109–114, 2009.

AZIZ, Shuokr Qarani et al. Leachate characterization in semi-aerobic and anaerobic sanitary landfills: A comparative study. **Journal of Environmental Management**, [s. l.], v. 91, n. 12, p. 2608–2614, 2010.

BADERNA, Diego; CALONI, Francesca; BENFENATI, Emilio. Investigating land fi ll leachate toxicity in vitro : A review of cell models and endpoints. [s. l.], n. November, 2018.

BADERNA, Diego; CALONI, Francesca; BENFENATI, Emilio. Investigating landfill leachate toxicity in vitro: A review of cell models and endpoints. **Environment International**, [s. l.], v. 122, p. 21–30, 2019.

BAIJU, Archa et al. Combined heterogeneous Electro-Fenton and biological process for the treatment of stabilized landfill leachate. **Journal of Environmental Management**, [s. l.], v. 210, p. 328–337, 2018.

BAKEN, Kirsten A. et al. A strategy to validate a selection of human effect biomarkers using adverse outcome pathways: Proof of concept for phthalates and reproductive effects. **Environmental Research**, [s. l.], v. 175, p. 235–256, 2019.

BASHIR, Mohammed J. K. et al. An overview of electro-oxidation processes performance in stabilized landfill leachate treatment. **Desalination and Water Treatment**, [s. l.], v. 51, n. 10–12, p. 2170–2184, 2013.

BENITO, Aleix et al. Degradation pathways of aniline in aqueous solutions during electro-oxidation with BDD electrodes and UV/H2O2 treatment. **Chemosphere**, [s. l.], v. 166, p. 230–237, 2017.

BIELSKI, Benon H. J. et al. Reactivity of HO2/O−2 Radicals in Aqueous Solution. **Journal of Physical and Chemical Reference Data**, [s. l.], v. 14, n. 4, p. 1041–1100, 1985.

BING, Xiaoyun et al. Research challenges in municipal solid waste logistics management. **Waste Management**, [s. l.], v. 48, p. 584–592, 2016.

BORBA, F. H. et al. Desirability function applied to the optimization of the Photoperoxi-Electrocoagulation process conditions in the treatment of tannery industrial wastewater. **Journal of Water Process Engineering**, [s. l.], v. 23, 2018.

BORBA, F. H. et al. Pollutant removal and acute toxicity assessment (Artemia salina) of landfill leachate treated by photo-Fenton process mediated by oxalic acid. **Journal of Water Process Engineering**, [s. l.], v. 28, 2019.

BRASIL. **Lei nº 12.305, de 02 de agosto 2010. Política Nacional de Resíduos Sólidos.** Brasília, 2010.

BRASIL. Resolução CONAMA Nº 430, de 13 de maio de 2011. Brasília. 2011.

BRILLAS, Enric; SIRÉS, Ignasi; OTURAN, Mehmet A. Electro-Fenton Process and Related Electrochemical Technologies Based on Fenton's Reaction Chemistry. **Chemical Reviews**, [s. l.], p. 6570–6631, 2009.

BRINZILA, C. I. et al. Electrodegradation of tetracycline on BDD anode. **Chemical Engineering Journal**, [s. l.], v. 209, p. 54–61, 2012.

BUDI, Setia et al. Toxicity identification evaluation of landfill leachate using fish, prawn and seed plant. **Waste Management**, [s. l.], v. 55, p. 231–237, 2016.

BUXTON, George V et al. Critical Review of rate constants for reactions of hydrated electrons, hydrogen atoms and hydroxyl radicals (·OH/·O− in Aqueous Solution. **Journal of Physical and Chemical Reference Data**, [s. l.], v. 17, n. 2, p. 513–886, 1988.

CAI, Jingju et al. Degradation of 2,4-dichlorophenoxyacetic acid by anodic oxidation and electro-Fenton using BDD anode: Influencing factors and mechanism. **Separation and Purification Technology**, [s. l.], v. 230, p. 115867, 2020.

CAÑIZARES, Pablo et al. Electrochemical treatment of diluted cyanide aqueous wastes. **Journal of Chemical Technology & Biotechnology**, [s. l.], v. 80, n. 5, p. 565–573, 2005.

CANLE, Moisés; FERNÁNDEZ PÉREZ, M. Isabel; SANTABALLA, J. Arturo. Photocatalyzed degradation/abatement of endocrine disruptors. **Current Opinion in Green and Sustainable Chemistry**, [s. l.], v. 6, p. 101–138, 2017.

CASSANO, D. et al. Comparison of several combined/integrated biological-AOPs setups for the treatment of municipal landfill leachate: Minimization of operating costs and effluent toxicity. **Chemical Engineering Journal**, [s. l.], v. 172, n. 1, p. 250–257, 2011.

CAVALCANTI, Eliane Bezerra et al. Electrochemical incineration of omeprazole in neutral aqueous medium using a platinum or boron-doped diamond anode:

Degradation kinetics and oxidation products. **Water Research**, [s. l.], v. 47, n. 5, p. 1803–1815, 2013.

CHEBI. **ChEBI database**. 2019. Disponível em: <https://www.ebi.ac.uk/chebi/searchId.do?chebiId=CHEBI:31725>. Acesso em: 10 jun. 2019.

CHEMLAL, R. et al. Combination of advanced oxidation and biological processes for the landfill leachate treatment. **Ecological Engineering**, [s. l.], v. 73, p. 281–289, 2014.

CHRISTENSEN, Hilbert; SEHESTED, Knud; CORFITZEN, Hanne. Reactions of hydroxyl radicals with hydrogen peroxide at ambient and elevated temperatures. **The Journal of Physical Chemistry**, [s. l.], v. 86, n. 9, p. 1588–1590, 1982.

DA SILVA, Salatiel W. et al. Using p-Si/BDD anode for the electrochemical oxidation of norfloxacin. **Journal of Electroanalytical Chemistry**, [s. l.], v. 832, p. 112–120, 2019. a.

DA SILVA, Salatiel Wohlmuth et al. Electrochemical advanced oxidation of Atenolol at Nb/BDD thin film anode. **Journal of Electroanalytical Chemistry**, [s. l.], v. 844, p. 27–33, 2019. b.

DAS, Subhasish et al. Solid waste management: Scope and the challenge of sustainability. **Journal of Cleaner Production**, [s. l.], v. 228, p. 658–678, 2019.

DAVIES, Peter Spencer. The biological basis of wastewater treatment. **Strathkelvin Instruments Ltd**, [s. l.], v. 3, 2005.

DE LAAT, Joseph; GALLARD, HervÉ. Catalytic Decomposition of Hydrogen Peroxide by Fe(III) in Homogeneous Aqueous Solution: Mechanism and Kinetic Modeling. **Environmental Science & Technology**, [s. l.], v. 33, n. 16, p. 2726–2732, 1999.

DE LAAT, Joseph; TRUONG LE, Giang; LEGUBE, Bernard. A comparative study of the effects of chloride, sulfate and nitrate ions on the rates of decomposition of H2O2 and organic compounds by Fe(II)/H2O2 and Fe(III)/H2O2. **Chemosphere**, [s. l.], v. 55, n. 5, p. 715–723, 2004.

DE MORAIS, Josmaria Lopes; ZAMORA, Patricio Peralta. Use of advanced oxidation

processes to improve the biodegradability of mature landfill leachates. **Journal of Hazardous Materials**, [s. l.], v. 123, n. 1–3, p. 181–186, 2005.

DE PAULI, Aline Roberta et al. New insights on abatement of organic matter and reduction of toxicity from landfill leachate treated by the electrocoagulation process. **Journal of Environmental Chemical Engineering**, [s. l.], v. 5, n. 6, p. 5448–5459, 2017.

DE PAULI, Aline Roberta et al. Integrated two-phase purification procedure for abatement of pollutants from sanitary landfill leachates. **Chemical Engineering Journal**, [s. l.], v. 334, p. 19–29, 2018.

DENG, Yang et al. Research on the treatment of biologically treated landfill leachate by joint electrochemical system. **Waste Management**, [s. l.], v. 82, p. 177–187, 2018.

DENG, Yang; ENGLEHARDT, James D. Treatment of landfill leachate by the Fenton process. **Water Research**, [s. l.], v. 40, n. 20, p. 3683–3694, 2006.

DEUS, Rafael Mattos; BATTISTELLE, Rosane Aparecida Gomes; SILVA, Gustavo Henrique Ribeiro. Current and future environmental impact of household solid waste management scenarios for a region of Brazil: carbon dioxide and energy analysis. **Journal of Cleaner Production**, [s. l.], v. 155, p. 218–228, 2017.

DEZZOTI, Marcia; LIPPEL, Geraldo; BASSIN, João Paulo. **Advanced Biological Processes for Wastewater Treatment: Emerging, Consolidated Technologies and Introduction to Molecular Technique**. 1. ed. [s.l: s.n.].

DIA, Oumar et al. Electrocoagulation of bio-filtrated landfill leachate: Fractionation of organic matter and influence of anode materials. **Chemosphere**, [s. l.], v. 168, p. 1136–1141, 2017.

DÍEZ, A. M. et al. Optimization of two-chamber photo electro Fenton reactor for the treatment of winery wastewater. **Process Safety and Environmental Protection**, [s. l.], v. 101, p. 72–79, 2016.

DIVYAPRIYA, Govindaraj; NAMBI, Indumathi; SENTHILNATHAN, Jaganathan. Ferrocene functionalized graphene based electrode for the electro−Fenton oxidation of ciprofloxacin. **Chemosphere**, [s. l.], v. 209, p. 113–123, 2018.

ECHA. **Chemicals inventory database**. 2019. Disponível em: <https://echa.europa.eu>.

EDJABOU, Maklawe Essonanawe et al. Municipal solid waste composition: Sampling methodology, statistical analyses, and case study evaluation. **Waste Management**, [s. l.], v. 36, p. 12–23, 2015.

EL-GHENYMY, Abdellatif et al. Electro-Fenton and photoelectro-Fenton degradation of the antimicrobial sulfamethazine using a boron-doped diamond anode and an air-diffusion cathode. **Journal of Electroanalytical Chemistry**, [s. l.], v. 701, p. 7–13, 2013.

EU. COMMISSION IMPLEMENTING REGULATION (EU) No 872/2012. 2012.

FAUST, Bruce C.; ZEPP, Richard G. Photochemistry of aqueous iron(III)-polycarboxylate complexes: roles in the chemistry of atmospheric and surface waters. **Environmental Science & Technology**, [s. l.], v. 27, n. 12, p. 2517–2522, 1993.

FENTON, H. J. H. Oxidation of tartaric acid in presence of iron. **Journal of the Chemical Society, Transactions**, [s. l.], v. 65, p. 899–910, 1894.

FERNANDES, A. et al. Anodic oxidation of a biologically treated leachate on a boron-doped diamond anode. **Journal of Hazardous Materials**, [s. l.], v. 199–200, p. 82–87, 2012.

FISKESJÖ, Geirid. The allium test in wastewater monitoring. **Environmental Toxicology and Water Quality**, [s. l.], v. 8, n. 3, p. 291–298, 1993.

FLOX, Cristina et al. Electrochemical incineration of cresols: A comparative study between PbO 2 and boron-doped diamond anodes. **Chemosphere**, [s. l.], v. 74, n. 10, p. 1340–1347, 2009.

FOLLER, P. C.; BOMBARD, R. T. Processes for the production of mixtures of caustic soda and hydrogen peroxide via the reduction of oxygen. **Journal of Applied Electrochemistry**, [s. l.], v. 25, n. 7, p. 613–627, 1995.

GALLARD, Herve′; DE LAAT, Joseph; LEGUBE, Bernard. Influence du pH sur la vitesse d’oxydation de compose′s organiques par FeII/H2O2. Me′canismes re′actionnels et mode′lisation. **New Journal of Chemistry**, [s. l.], v. 22, n. 3, p. 263–

268, 1998.

GALLEGOS, Alberto Alvarez; GARCÍA, Yary Vergara; ZAMUDIO, Alvaro. Solar hydrogen peroxide. **Solar Energy Materials and Solar Cells**, [s. l.], v. 88, n. 2, p. 157–167, 2005.

GANIYU, Soliu O.; ZHOU, Minghua; MARTÍNEZ-HUITLE, Carlos A. Heterogeneous electro-Fenton and photoelectro-Fenton processes: A critical review of fundamental principles and application for water/wastewater treatment. **Applied Catalysis B: Environmental**, [s. l.], v. 235, p. 103–129, 2018.

GARCIA-SEGURA, Sergi; BRILLAS, Enric. Advances in solar photoelectro-Fenton: Decolorization and mineralization of the Direct Yellow 4 diazo dye using an autonomous solar pre-pilot plant. **Electrochimica Acta**, [s. l.], v. 140, p. 384–395, 2014.

GRADY JR, C. P. Leslie et al. **Biological Wastewater Treatment**. 3. ed. [s.l.] : IWA Publishing, 2011.

GUO, Jin-Song et al. Treatment of landfill leachate using a combined stripping, Fenton, SBR, and coagulation process. **Journal of Hazardous Materials**, [s. l.], v. 178, n. 1–3, p. 699–705, 2010.

GUPTA, Abhinav et al. Variation in organic matter characteristics of landfill leachates in different stabilisation stages. **Waste Management & Research**, [s. l.], v. 32, n. 12, p. 1192–1199, 2014.

HABER, Fritz; WEISS, Joseph. The Catalytic Decomposition of Hydrogen Peroxide by Iron Salts. **Proceedings of the Royal Society of London. Series A, Mathematical and Physical Sciences**, [s. l.], v. 147, n. 861, p. 332–351, 1934.

HAMZA, Morched et al. Comparative electrochemical degradation of the triphenylmethane dye Methyl Violet with boron-doped diamond and Pt anodes. **Journal of Electroanalytical Chemistry**, [s. l.], v. 627, n. 1–2, p. 41–50, 2009.

HENZE, M. et al. **Biological Wastewater Treatment: Principles, Modelling and Design**IWA Publishing, , 2008.

HSDB. **Diisooctyl phthalate. National Library of Medicine HSDB Database**. 2019.

Disponível em: <https://toxnet.nlm.nih.gov/cgi-bin/sis/search2/f?./temp/~Y3Fyyz:2>.

HU, Liang et al. Treatment of landfill leachate using immobilized Phanerochaete chrysosporium loaded with nitrogen-doped TiO2 nanoparticles. **Journal of Hazardous Materials**, [s. l.], v. 301, p. 106–118, 2016.

INGLEZAKIS, V. J. et al. Treatment of municipal solid waste landfill leachate by use of combined biological, physical and photochemical processes. **Desalination and Water Treatment**, [s. l.], v. 112, p. 218–231, 2018.

JARDIM, WILSON F.; CANELA, MARIA CRISTINA. Fundamentos da oxidação química no tratamento de efluentes e remediação de solos. **UNICAMP. Campinas**, [s. l.], 2004.

KANNO, Sanae; FURUYAMA, Akiko; HIRANO, Seishiro. Effects of eicosane, a component of nanoparticles in diesel exhaust, on surface activity of pulmonary surfactant monolayers. **Archives of Toxicology**, [s. l.], v. 82, n. 11, p. 841–850, 2008.

KAPELEWSKA, Justyna; KOTOWSKA, Urszula; WIŚNIEWSKA, Katarzyna. Determination of personal care products and hormones in leachate and groundwater from Polish MSW landfills by ultrasound-assisted emulsification microextraction and GC-MS. **Environmental Science and Pollution Research**, [s. l.], v. 23, n. 2, p. 1642–1652, 2016.

KAZA, Silpa et al. **What a Waste 2.0: A Global Snapshot of Solid Waste Management to 2050**. [s.l.] : World Bank Publications, 2018.

KHALIL, Christian et al. Municipal leachates health risks: Chemical and cytotoxicity assessment from regulated and unregulated municipal dumpsites in Lebanon. **Chemosphere**, [s. l.], v. 208, p. 1–13, 2018.

KHAN, Sheeba; FAISAL, Mohd Nishat. An analytic network process model for municipal solid waste disposal options. **Waste Management**, [s. l.], v. 28, n. 9, p. 1500–1508, 2008.

KHATRI, Inderjeet; SINGH, Swati; GARG, Anurag. Performance of electro-Fenton process for phenol removal using Iron electrodes and activated carbon. **Journal of Environmental Chemical Engineering**, [s. l.], v. 6, n. 6, p. 7368–7376, 2018.

KIM, Soo-M.; GEISSEN, Sven-U.; VOGELPOHL, Alfons. Landfill leachate treatment by a photoassisted fenton reaction. **Water Science and Technology**, [s. l.], v. 35, n. 4, p. 239–248, 1997.

KLAUCK, C. R.; RODRIGUES, M. A. S.; SILVA, L. B. **Evaluation of phytotoxicity of municipal landfill leachate before and after biological treatment Brazilian Journal of Biology** scielo, 2015.

KLAUCK, Cláudia Regina et al. Toxicity elimination of landfill leachate by hybrid processing of advanced oxidation process and adsorption. **Environmental Technology & Innovation**, [s. l.], v. 8, p. 246–255, 2017.

KULIKOWSKA, Dorota; KLIMIUK, Ewa. The effect of landfill age on municipal leachate composition. **Bioresource Technology**, [s. l.], v. 99, n. 13, p. 5981–5985, 2008.

KURNIAWAN, Tonni Agustiono et al. Biological processes for treatment of landfill leachate. **Journal of Environmental Monitoring**, [s. l.], v. 12, n. 11, p. 2032–2047, 2010.

LAPERTOT, Milena Eleonore; PULGARIN, Cesar. Biodegradability assessment of several priority hazardous substances: Choice, application and relevance regarding toxicity and bacterial activity. **Chemosphere**, [s. l.], v. 65, n. 4, p. 682–690, 2006.

LEE, Tzong-Huei et al. Heptadecanols from the leaves of Persea americana var. americana. **Food Chemistry**, [s. l.], v. 132, n. 2, p. 921–924, 2012.

LEI, Yangming et al. Treatment of landfill leachate by combined aged-refuse bioreactor and electro-oxidation. **Water Research**, [s. l.], v. 41, n. 11, p. 2417–2426, 2007.

LEME, Daniela Morais; MARIN-MORALES, Maria Aparecida. Allium cepa test in environmental monitoring: A review on its application. **Mutation Research/Reviews in Mutation Research**, [s. l.], v. 682, n. 1, p. 71–81, 2009.

LIU, Xiaocheng et al. Insight into electro-Fenton and photo-Fenton for the degradation of antibiotics: Mechanism study and research gaps. **Chemical Engineering Journal**, [s. l.], v. 347, p. 379–397, 2018.

LIU, Ze hua; YIN, Hua; DANG, Zhi. Do estrogenic compounds in drinking water migrating from plastic pipe distribution system pose adverse effects to human? An

analysis of scientific literature. **Environmental Science and Pollution Research**, [s. l.], v. 24, n. 2, p. 2126–2134, 2017.

LOPEZ, Antonio et al. Fenton's pre-treatment of mature landfill leachate. **Chemosphere**, [s. l.], v. 54, n. 7, p. 1005–1010, 2004.

LÖSCHNER, Dorit et al. Experience with the application of the draft European Standard prEN 15768 to the identification of leachable organic substances from materials in contact with drinking water by GC-MS. **Analytical Methods**, [s. l.], v. 3, n. 11, p. 2547–2556, 2011.

LOUHICHI, B. et al. Electrochemical degradation of an anionic surfactant on boron-doped diamond anodes. **Journal of Hazardous Materials**, [s. l.], v. 158, n. 2–3, p. 430–437, 2008.

MADIGAN, Michael T. et al. **Microbiologia de Brock**. 14. ed. Porto Alegre.

MAIA, Iracema Souza et al. Avaliação do tratamento biológico de lixiviado de aterro sanitário em escala real na Região Sul do Brasil. **Engenharia Sanitaria e Ambiental**, [s. l.], v. 20, n. 4, p. 665–675, 2015.

MALATO, Sixto et al. Photocatalytic decontamination and disinfection of water with solar collectors. **Catalysis Today**, [s. l.], v. 122, n. 1–2, p. 137–149, 2007.

MANDAL, Pubali; DUBEY, Brajesh K.; GUPTA, Ashok K. Review on landfill leachate treatment by electrochemical oxidation: Drawbacks, challenges and future scope. **Waste Management**, [s. l.], v. 69, p. 250–273, 2017.

MARSELLI, Beatrice et al. Electrogeneration of hydroxyl radicals on boron-doped diamond electrodes. **Journal of the Electrochemical Society**, [s. l.], v. 150, n. 3, p. D79–D83, 2003.

MARTÍNEZ-HUITLE, Carlos A.; FERRO, Sergio. Electrochemical oxidation of organic pollutants for the wastewater treatment: Direct and indirect processes. **Chemical Society Reviews**, [s. l.], v. 35, n. 12, p. 1324–1340, 2006.

MAUERHOFER, Lisa-maria et al. **Methods for quantification of growth and productivity in anaerobic microbiology and biotechnology**. [s.l.] : Folia Microbiologica, 2019.

MIAN, Md Manik et al. Municipal solid waste management in China: a comparative analysis. **Journal of Material Cycles and Waste Management**, [s. l.], v. 19, n. 3, p. 1127–1135, 2017.

MOLLAH, M. Yousu. A. et al. Electrocoagulation (EC) — science and applications. **Journal of Hazardous Materials**, [s. l.], v. 84, n. 1, p. 29–41, 2001.

MOREIRA, Francisca C. et al. Degradation of trimethoprim antibiotic by UVA photoelectro-Fenton process mediated by Fe(III)–carboxylate complexes. **Applied Catalysis B: Environmental**, [s. l.], v. 162, p. 34–44, 2015. a.

MOREIRA, Francisca C. et al. Incorporation of electrochemical advanced oxidation processes in a multistage treatment system for sanitary landfill leachate. **Water Research**, [s. l.], v. 81, p. 375–387, 2015. b.

MOREIRA, Francisca C. et al. Electrochemical advanced oxidation processes: A review on their application to synthetic and real wastewaters. **Applied Catalysis B: Environmental**, [s. l.], v. 202, p. 217–261, 2017.

MOROZESK, Mariana et al. Effects of humic acids from landfill leachate on plants: An integrated approach using chemical, biochemical and cytogenetic analysis. **Chemosphere**, [s. l.], v. 184, p. 309–317, 2017.

NAVEEN, B. P. et al. Physico-chemical and biological characterization of urban municipal landfill leachate. **Environmental Pollution**, [s. l.], v. 220, p. 1–12, 2017.

NEDELKOSKA, T. V.; DORAN, P. M. Characteristics of heavy metal uptake by plant species with potential for phytoremediation and phytomining. **Minerals Engineering**, [s. l.], v. 13, n. 5, p. 549–561, 2000.

NIDHEESH, P. V.; GANDHIMATHI, R. Trends in electro-Fenton process for water and wastewater treatment: An overview. **Desalination**, [s. l.], v. 299, p. 1–15, 2012.

NOGUEIRA, Raquel F. Pupo; OLIVEIRA, Mirela C.; PATERLINI, Willian C. Simple and fast spectrophotometric determination of H2O2 in photo-Fenton reactions using metavanadate. **Talanta**, [s. l.], v. 66, n. 1, p. 86–91, 2005.

OCHIAI, Tsuyoshi et al. Efficient electrochemical decomposition of perfluorocarboxylic acids by the use of a boron-doped diamond electrode. **Diamond and Related**

Materials, [s. l.], v. 20, n. 2, p. 64–67, 2011.

OLLER, I. et al. A combined solar photocatalytic-biological field system for the mineralization of an industrial pollutant at pilot scale. **Catalysis Today**, [s. l.], v. 122, n. 1–2, p. 150–159, 2007.

OLLER, I.; MALATO, S.; SÁNCHEZ-PÉREZ, J. A. Combination of Advanced Oxidation Processes and biological treatments for wastewater decontamination—A review. **Science of The Total Environment**, [s. l.], v. 409, n. 20, p. 4141–4166, 2011.

ÖMAN, Cecilia B.; JUNESTEDT, Christian. Chemical characterization of landfill leachates - 400 parameters and compounds. **Waste Management**, [s. l.], v. 28, n. 10, p. 1876–1891, 2008.

PANIZZA, M.; CERISOLA, G. Application of diamond electrodes to electrochemical processes. **Electrochimica Acta**, [s. l.], v. 51, n. 2, p. 191–199, 2005.

PANIZZA, Marco; CERISOLA, Giacomo. Electrochemical Degradation of Methyl Red Using BDD and PbO2 Anodes. **Industrial & Engineering Chemistry Research**, [s. l.], v. 47, n. 18, p. 6816–6820, 2008.

PANIZZA, Marco; CERISOLA, Giacomo. Direct And Mediated Anodic Oxidation of Organic Pollutants. **Chemical Reviews**, [s. l.], v. 109, n. 12, p. 6541–6569, 2009.

PENG, Yao. Perspectives on technology for landfill leachate treatment. **Arabian Journal of Chemistry**, [s. l.], v. 10, p. S2567–S2574, 2017.

PEREIRA, Gabriel F. et al. Effective removal of Orange-G azo dye from water by electro-Fenton and photoelectro-Fenton processes using a boron-doped diamond anode. **Separation and Purification Technology**, [s. l.], v. 160, p. 145–151, 2016.

PÉREZ, Montserrat et al. Fenton and photo-Fenton oxidation of textile effluents. **Water Research**, [s. l.], v. 36, n. 11, p. 2703–2710, 2002.

PIGNATELLO, Joseph J. Dark and photoassisted iron(3+)-catalyzed degradation of chlorophenoxy herbicides by hydrogen peroxide. **Environmental Science & Technology**, [s. l.], v. 26, n. 5, p. 944–951, 1992.

PIGNATELLO, Joseph J.; OLIVEROS, Esther; MACKAY, Allison. Advanced Oxidation

Processes for Organic Contaminant Destruction Based on the Fenton Reaction and Related Chemistry. **Critical Reviews in Environmental Science and Technology**, [s. l.], v. 36, n. 1, p. 1–84, 2006.

RA, Jin-Sung et al. Application of toxicity identification evaluation procedure to toxic industrial effluent in South Korea. **Chemosphere**, [s. l.], v. 143, p. 71–77, 2016.

RAMÍREZ, Cecilia et al. Electrochemical oxidation of methyl orange azo dye at pilot flow plant using BDD technology. **Journal of Industrial and Engineering Chemistry**, [s. l.], v. 19, n. 2, p. 571–579, 2013.

REN, Yanan et al. Comparing young landfill leachate treatment efficiency and process stability using aerobic granular sludge and suspended growth activated sludge. **Journal of Water Process Engineering**, [s. l.], v. 17, p. 161–167, 2017.

RENOU, S. et al. Landfill leachate treatment: Review and opportunity. **Journal of Hazardous Materials**, [s. l.], v. 150, n. 3, p. 468–493, 2008.

RICE, Eugene W.; PUBLIC HEALTH ASSOCIATION, American. **Standard methods for the examination of water and wastewater**. [s.l: s.n.].

RUSH, James D.; BIELSKI, Benon H. J. Pulse radiolytic studies of the reaction of perhydroxyl/superoxide O2- with iron(II)/iron(III) ions. The reactivity of HO2/O2- with ferric ions and its implication on the occurrence of the Haber-Weiss reaction. **The Journal of Physical Chemistry**, [s. l.], v. 89, n. 23, p. 5062–5066, 1985.

SAŁEK, Karina; EUSTON, Stephen R. Sustainable microbial biosurfactants and bioemulsifiers for commercial exploitation. **Process Biochemistry**, [s. l.], v. 85, p. 143–155, 2019.

SANG, Nan; LI, Guangke; XIN, Xiaoyun. Municipal landfill leachate induces cytogenetic damage in root tips of Hordeum vulgare. **Ecotoxicology and Environmental Safety**, [s. l.], v. 63, n. 3, p. 469–473, 2006.

SEIBERT, Daiana et al. Presence of endocrine disrupting chemicals in sanitary landfill leachate , its treatment and degradation by Fenton based processes : A review. **Process Safety and Environmental Protection**, [s. l.], v. 131, p. 255–267, 2019. a.

SEIBERT, Daiana et al. Two-stage integrated system photo-electro-Fenton and

biological oxidation process assessment of sanitary landfill leachate treatment: An intermediate products study. **Chemical Engineering Journal**, [s. l.], v. 372, p. 471–482, 2019. b.

SERDAREVIC, Amra. Landfill Leachate Management — Control and Treatment. **Advanced Technologies, Systems, and Applications II**, [s. l.], p. pp 618-632, 2018.

SILVA, Tânia F. C. V. et al. Multistage treatment system for raw leachate fromsanitary landfill combining biological nitrification-denitrification/solar photo-Fenton/biological processes, at a scale close to industrial - Biodegradability enhancement and evolution profile of trace pol. **Water Research**, [s. l.], v. 47, n. 16, p. 6167–6186, 2013.

SILVA, Tânia F. C. V. et al. Scale-up and cost analysis of a photo-Fenton system for sanitary landfill leachate treatment. **Chemical Engineering Journal**, [s. l.], v. 283, p. 76–88, 2016.

SIRÉS, Ignasi et al. Comparative depollution of mecoprop aqueous solutions by electrochemical incineration using BDD and PbO2 as high oxidation power anodes. **Journal of Electroanalytical Chemistry**, [s. l.], v. 613, n. 2, p. 151–159, 2008.

SIRÉS, Ignasi et al. Electrochemical advanced oxidation processes: Today and tomorrow. A review. **Environmental Science and Pollution Research**, [s. l.], v. 21, n. 14, p. 8336–8367, 2014.

SOBRERO, Maria Cecilia; RONCO, Alicia. Ensayo de toxicidad aguda con semillas de lechuga (Lactuca sativa L.). **Ensayos toxicológicos ymétodos de evaluación de calidad de aguas: standerización, intercalibración, resultados y aplicaciones. Mexico: IMTA**, [s. l.], 2004.

SRUTHI, T. et al. Stabilized landfill leachate treatment using heterogeneous Fenton and electro-Fenton processes. **Chemosphere**, [s. l.], v. 210, p. 38–43, 2018.

SUI, Qian et al. Occurrence and removal of pharmaceuticals, caffeine and DEET in wastewater treatment plants of Beijing, China. **Water Research**, [s. l.], v. 44, n. 2, p. 417–426, 2010.

SUN, Yunfu; PIGNATELLO, Joseph J. Photochemical reactions involved in the total mineralization of 2,4-D by iron(3+)/hydrogen peroxide/UV. **Environmental Science &**

Technology, [s. l.], v. 27, n. 2, p. 304–310, 1993.

UDDIN, Shaikh Jamal; GRICE, Darren; TIRALONGO, Evelin. Evaluation of cytotoxic activity of patriscabratine, tetracosane and various flavonoids isolated from the Bangladeshi medicinal plant Acrostichum aureum. **Pharmaceutical Biology**, [s. l.], v. 50, n. 10, p. 1276–1280, 2012.

UMAR, Muhammad; AZIZ, Hamidi Abdul; YUSOFF, Mohd Suffian. Trends in the use of Fenton, electro-Fenton and photo-Fenton for the treatment of landfill leachate. **Waste Management**, [s. l.], v. 30, n. 11, p. 2113–2121, 2010.

USEPA. **Endocrine Disruptor Screening Program**. [s.l: s.n.].

VILAR, Vítor J. P. et al. Treatment of a sanitary landfill leachate using combined solar photo-Fenton and biological immobilized biomass reactor at a pilot scale. **Water Research**, [s. l.], v. 45, n. 8, p. 2647–2658, 2011.

WANG, Chih-Ta et al. COD removal from real dyeing wastewater by electro-Fenton technology using an activated carbon fiber cathode. **Desalination**, [s. l.], v. 253, n. 1–3, p. 129–134, 2010.

WANG, Nannan et al. A review on Fenton-like processes for organic wastewater treatment. **Journal of Environmental Chemical Engineering**, [s. l.], v. 4, n. 1, p. 762–787, 2016.

WELCH, Ross M.; SHUMAN, Larry. Micronutrient Nutrition of Plants Critical Reviews in Plant Sciences Micronutrient Nutrition of Plants. **Critical Reviews in Plant Sciences**, [s. l.], n. November, p. 37–41, 1995.

WELTER, Júlia Bitencourt et al. Bioassays and Zahn-Wellens test assessment on landfill leachate treated by photo-Fenton process. **Journal of Environmental Chemical Engineering**, [s. l.], v. 6, n. 1, p. 1390–1395, 2018.

XIAO, Shuhu et al. Degradation of biologically treated landfill leachate by using electrochemical process combined with UV irradiation. **Separation and Purification Technology**, [s. l.], v. 117, p. 24–29, 2013.

XU, Lejin; WANG, Jianlong. A heterogeneous Fenton-like system with nanoparticulate zero-valent iron for removal of 4-chloro-3-methyl phenol. **Journal of Hazardous**

Materials, [s. l.], v. 186, n. 1, p. 256–264, 2011.

YAZICI GUVENC, Senem; DINCER, Kaan; VARANK, Gamze. Performance of electrocoagulation and electro-Fenton processes for treatment of nanofiltration concentrate of biologically stabilized landfill leachate. **Journal of Water Process Engineering**, [s. l.], v. 31, p. 100863, 2019.

ZAZOULI, Mohammad Ali et al. Municipal solid waste landfill leachate treatment by Fenton, photo-Fenton and Fenton-like processes: Effect of some variables. **Iranian Journal of Environmental Health Science and Engineering**, [s. l.], v. 9, n. 3, 2012.

ZHANG, Guoliang et al. Aerobic SMBR/reverse osmosis system enhanced by Fenton oxidation for advanced treatment of old municipal landfill leachate. **Bioresource Technology**, [s. l.], v. 142, p. 261–268, 2013.

ZHANG, Hui et al. Evaluation of electro-oxidation of biologically treated landfill leachate using response surface methodology. **Journal of Hazardous Materials**, [s. l.], v. 188, n. 1–3, p. 261–268, 2011.

ZHANG, Hui; CHOI, Heung Jin; HUANG, Chin-Pao. Optimization of Fenton process for the treatment of landfill leachate. **Journal of Hazardous Materials**, [s. l.], v. 125, n. 1–3, p. 166–174, 2005.

ZHU, Xiuping et al. Destination of organic pollutants during electrochemical oxidation of biologically-pretreated dye wastewater using boron-doped diamond anode. **Journal of Hazardous Materials**, [s. l.], v. 189, n. 1–2, p. 127–133, 2011.

ZHUANG, Yuan et al. Structural transformation and potential toxicity of iron-based deposits in drinking water distribution systems. **Water Research**, [s. l.], v. 165, p. 114999, 2019.

ZHUO, Qiongfang et al. Electrochemical oxidation of perfluorooctane sulfonate (PFOS) substitute by modified boron doped diamond (BDD) anodes. **Chemical Engineering Journal**, [s. l.], v. 379, p. 122280, 2020.

ZIYANG, Lou et al. Natural attenuation and characterization of contaminants composition in landfill leachate under different disposing ages. **Science of the Total Environment**, [s. l.], v. 407, n. 10, p. 3385–3391, 2009.

ZOLFAGHARI, Mehdi et al. Landfill leachate treatment by sequential membrane bioreactor and electro-oxidation processes. **Journal of Environmental Management**, [s. l.], v. 184, p. 318–326, 2016.

ZUO, Yuegang; HOIGNE, Juerg. Formation of hydrogen peroxide and depletion of oxalic acid in atmospheric water by photolysis of iron(III)-oxalato complexes. **Environmental Science & Technology**, [s. l.], v. 26, n. 5, p. 1014–1022, 1992.